

## COMMENTARY

# Seeing is believing – multi-scale spatio-temporal imaging towards *in vivo* cell biology

Gautier Follain<sup>1,2,3,4,\*</sup>, Luc Mercier<sup>1,2,3,4,\*</sup>, Naël Osmani<sup>1,2,3,4,\*</sup>, Sébastien Harlepp<sup>2,5,6,\*</sup> and Jacky G. Goetz<sup>1,2,3,4,†</sup>

## ABSTRACT

Life is driven by a set of biological events that are naturally dynamic and tightly orchestrated from the single molecule to entire organisms. Although biochemistry and molecular biology have been essential in deciphering signaling at a cellular and organismal level, biological imaging has been instrumental for unraveling life processes across multiple scales. Imaging methods have considerably improved over the past decades and now allow to grasp the inner workings of proteins, organelles, cells, organs and whole organisms. Not only do they allow us to visualize these events in their most-relevant context but also to accurately quantify underlying biomechanical features and, so, provide essential information for their understanding. In this Commentary, we review a palette of imaging (and biophysical) methods that are available to the scientific community for elucidating a wide array of biological events. We cover the most-recent developments in intravital imaging, light-sheet microscopy, super-resolution imaging, and correlative light and electron microscopy. In addition, we illustrate how these technologies have led to important insights in cell biology, from the molecular to the whole-organism resolution. Altogether, this review offers a snapshot of the current and state-of-the-art imaging methods that will contribute to the understanding of life and disease.

**KEY WORDS:** Cell biology, Imaging, *In vivo* imaging, 1PEM, 2PEM, CLEM, LSFM, SIM, SPIM, STED microscopy

## Introduction

Understanding complex and integrated cellular behaviors can be performed at various levels. The post-genomic era led to the development of numerous ‘omics’ efforts with the ambitious goal of predicting and, thereby, anticipating the treatment of clinical phenotypes by integrating multi-scale information from the patient. This concept of personalized and precision medicine faces the challenge to integrate the extremely large amount of available ‘omics’ biomedical data for the development of personalized treatments to cure patients in a routine day-to-day clinical practice. Cell biology is playing a main role in the understanding of clinical phenotype at a cellular scale. Performing *in vivo* cell biology aims to understand a disease at a subcellular scale and to integrate this information into the wider context of a tissue or an organ. Although

multi-omic approaches can grasp snapshots of a disease at multiple scales, they are often restricted to a selected time-point that does not fully represent the dynamics of cells and tissues. Thanks to the recent development of fast and high-resolution imaging approaches, *in vivo* models, gene editing, cell and biomaterial engineering, as well as high-throughput procedures, it is now possible to probe and understand – at multiple scales – the link between subcellular phenomenon and cell phenotype, both in normal or pathophysiological contexts. Because pathologies often emanate from subcellular and dynamic events that are then integrated in tissues, access to the full cellular organization is required, in 3D and in real-time, and within its most relevant context.

In this Commentary, we aim to provide a snapshot of existing as well as recent developments in live-cell imaging, which now makes the concept of *in vivo* cell biology a reachable target. Here, *in vivo* refers to imaging performed in whole living animals. Because animal models are central in understanding cellular phenotypes that are essential to development or disease progression, we start by summarizing the basics of intravital imaging, which aims to visualize an event of interest in its most representative biological context. We particularly emphasize recent developments in nonlinear microscopy, which offers means to image cellular and micro-environmental behaviors in a non-invasive manner. Because phototoxicity is an important criterium in performing live *in vivo* cell biology, we then summarize the recent development and latest improvements in light-sheet microscopy, which offers unprecedented information at the organismal scale for small animals. Cell biology is tightly linked to biomechanics and has led to the emergence of a widespread concept of mechanobiology that aims to unravel the contribution of mechanical forces to biological events and disease. We thus also provide a glimpse of the existing biophysical methods that can be applied to *in vivo* cell biology and highlight some of their applications (see Box 1). We continue by describing the recent developments in super-resolution imaging and illustrate the recent developments with some biological applications that clearly suggest that *in vivo* super-resolution can be reached within the next few years. Finally, because the highest resolution can still not be obtained on living animals, we conclude by discussing the recent progress made in correlative light and electron microscopy (CLEM), including in the area of intravital correlative microscopy, which offers access to high-resolution imaging of cellular events *in vivo*. We also provide a summary table that, for each technology, lists the advantages and limitations, the resolution that can be achieved, the technical difficulties and the key applications in cell biology (Table 1).

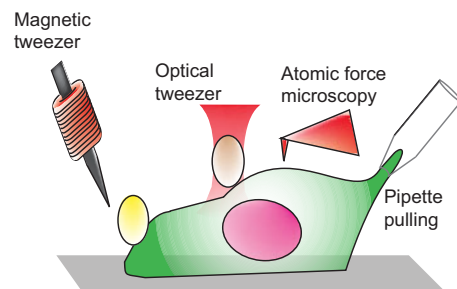
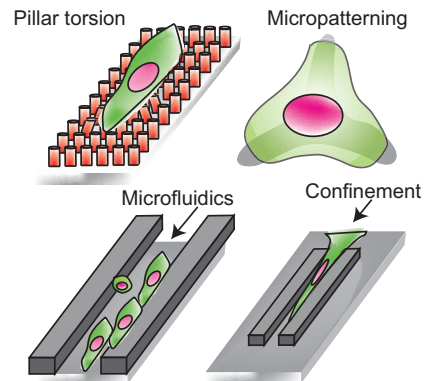
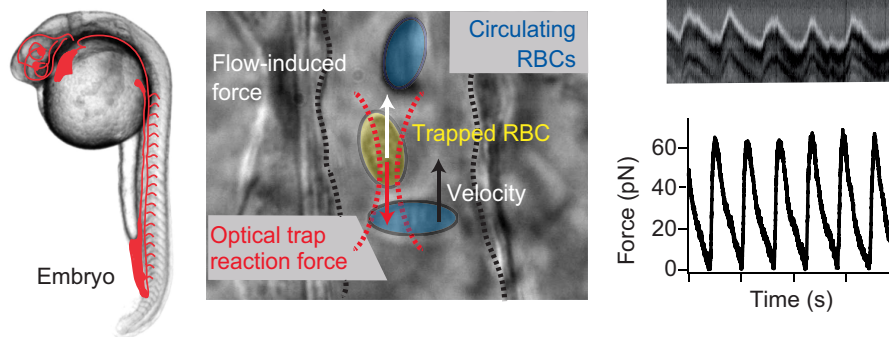
### Intravital imaging – tracking biological events *in vivo* within higher organisms

Dynamic visualization of biological processes in their natural environment is an important challenge for cell biologists. There is an obvious difference between the thickness of samples that are

<sup>1</sup>Microenvironmental Niche in Tumorigenesis and Targeted Therapy, Inserm U1109, MN3T, Strasbourg F-67200, France. <sup>2</sup>Université de Strasbourg, Strasbourg F-67000, France. <sup>3</sup>LabEx Medalis, Université de Strasbourg, Strasbourg, F-67000, France. <sup>4</sup>Fédération de Médecine Translationnelle de Strasbourg (FMTS), Strasbourg F-67000, France. <sup>5</sup>DON: Optique ultrarapide et nanophotonique, IPCMS UMR7504, Strasbourg 67000, France. <sup>6</sup>LabEx NIE, Université de Strasbourg, Strasbourg F-67000, France.

\*These authors contributed equally to this work

†Author for correspondence (jacky.goetz@inserm.fr)

**Box 1. A snapshot of the available biophysical tools for assessing cellular forces****A Manipulating tools****B Micropatterning tools****C Optical tweezers *in vivo***

In addition to imaging cell behavior, a wide palette of biophysical tools is available to cell biologists when assessing and quantifying cellular mechanical forces. Whereas these tools are mostly suited for assessing forces *in vitro* (for theoretical background, see e.g. Neuman and Nagy, 2008; Kim et al., 2009; Ahmed et al., 2015) (panels A and B), some can be applied *in vivo* and to offer detailed quantification of forces in living animals (panel C). (A) Magnetic tweezers originate from the interaction of a magnetic bead fixed to the cell membrane with a magnetic field gradient (Tanase et al., 2007; Salerno et al., 2010). Historically used *in vitro* to measure mechanical properties at the single molecule (Graves et al., 2015; Strick et al., 1996) or at the single cell level (Collins et al., 2014; Marjoram et al., 2016), magnetic tweezers have recently shown their efficacy in measuring forces *in vivo* during embryonic development (Brunet et al., 2013; Desprat et al., 2008). Optical tweezers require a strongly focused laser beam that generates a 3D trap, which behaves as a spring (Ashkin, 1997). This optical technique has originally been used for *in vitro* measurement of viscoelastic properties of single molecules (Klajnner et al., 2010; Smith et al., 1996) or single cells (Ashkin and Dziedzic, 1987; Ashkin et al., 1987; Dao et al., 2003). Recently, this technique has been applied *in vivo* for quantifying cell junction elasticity (Bambardekar et al., 2015; Sugimura et al., 2016) and proepicardial cell adhesion (Peralta et al., 2013), as well as for trapping circulating blood cells, thereby addressing haemodynamic forces in zebrafish (Anton et al., 2013) and mouse (Zhong et al., 2013). In atomic force microscopy (AFM), a cantilever is transiently brought in contact with the cell surface (Tartibi et al., 2015), cell nuclei (Lanzicher et al., 2015), or biological material such as cell-derived matrices (Tello et al., 2016). The analysis of its deflection over contact is linked to the exerted force and the mechanical response of the cell, which are mostly viscoelastic (Young modulus and viscosity). Even though this contact technique is mostly adapted to *in vitro* samples obtained either through cell culture (Kuznetsova et al., 2007; Ossola et al., 2015) or biopsies (Plodinec et al., 2012), AFM can be also used *in vivo*; for example, in mouse blood vessels (Mao et al., 2009). Micropipette pulling consists in locally aspirating the cell through a microforged pipette and in following the deformation for single cells (Guilak et al., 2000; Hochmuth, 2000; Chivukula et al., 2015) or for clusters of cells (Guevorkian et al., 2010, 2011). Traction force microscopy (Schwarz and Soiné, 2015) and pillar deformation (Khare et al., 2015) use calibrated soft substrates. Upon spreading, cells exert forces, which subsequently deform the substrate; these deformations inform about the localization and the amount of applied forces (Balaban et al., 2001; Gupta et al., 2015). (B) The development of improved micropatterning approaches allows the precise assessment of how surface topography influences the behavior of intracellular organelles or the cytoskeleton (Théry et al., 2006; Versaevél et al., 2012). The fast-evolving field of microfluidics has recently been used to assess how fluid forces (Perrault et al., 2015; Vartanian et al., 2008), mechanical confinement (Liu et al., 2015) or topological constrictions (Raab et al., 2016; Thiam et al., 2016) influence the behavior of cells. Measuring the migration time through confined 3D geometry provides information regarding cellular migration over topological constrictions (Thiam et al., 2016). Thus, when combined with imaging approaches, these biophysical tools offer a quantitative approach to the study of biomechanical events. (C) Optical tweezers can be applied *in vivo* on a zebrafish embryo. Focusing the laser spot in the vasculature allows the trapping of red blood cells (RBC). Pulsatility of the blood flow is visible upon kymographic analysis of the RBC displacement in the trap. This displacement is proportional to the drag force that RBCs are subjected to.

mounted on glass slides *in vitro* and whole living organisms. Here, intravital imaging refers to *in vivo* imaging within higher organisms, such as rats and mice. However, similar technologies can be used for imaging embryos and, thereby, can exploit the advantages provided by nonlinear microscopy (see below). The main drawback of conventional widefield microscopy applied to voluminous samples

is that it is impossible to provide clear and sharp images. Indeed, imaging quality within the focal plane is highly perturbed by out-of-plane scattered light. To circumvent this problem, Marvin Minsky developed – already more than fifty years ago – the first prototype of a confocal scanning microscope (Minsky, 1961). Modern confocal microscopes work on the principle of point scanning, whereby the

**Table 1. Pros and cons of current imaging technologies**

	1/2PEM	LSFM	Super Resolution	CLEM
Sample type	Fixed and/or live single cells up to higher organisms (mouse, rat)	Fixed and/or live single cells to embryos (ZF, fly, etc.)	Fixed and/or live single cells to embryos (ZF, fly, etc.)	Live to fixed sample Single cells to higher organisms (mouse, rat)
Resolution	200–2 nm	----->		
	Cellular to subcellular	Cellular to subcellular	Subcellular to single molecule	nanometer
Speed	High	High to very high	Low	Very low
Penetration	Very high when using 2PEM	High	Low	Limited by light microscopy
Data volume	Small	Large	Large for PALM/STORM Small for SIM and STED	Large
Technical difficulty	Animal handling under the microscope	Data acquisition and processing	Data processing for PALM/STORM and SIM	Finding the ROI again between imaging modalities, time-consuming
Main advantage	Most-established method, easy, versatile	Best compromise between resolution and speed ratio	Best localization (sub-diffraction limited)	Best overall resolution when combined with electron tomography
Specific feature	<b>1PEM:</b> Better resolution compared to widefield microscopy  <b>2PEM:</b> In-depth long-term imaging of mice, fluorescent imaging and label-free imaging	Long-term 3D imaging with high-speed or high 3D resolution  <b>SPIM:</b> Multiview imaging increases 3D acquisition speed  <b>DSLIM:</b> More suitable for super-resolution technologies	<b>STED:</b> Increased resolution for any 1PEM and 2PEM sample compatible with confocal imaging <b>SIM:</b> Fast 2D and 3D sub-diffraction imaging  <b>PALM/STORM:</b> single-molecule resolution, single-particle tracking	Compatible with any <i>in vivo</i> model  Requires manpower Requires access to sophisticated EM technologies for 3DEM
Biological application	Cancer biology, developmental biology, neurosciences, stem cell biology	Cell biology, developmental biology, neurosciences	Cell biology, developmental biology, neurosciences, biophysics	Cancer biology, developmental biology, neurosciences, stem cell biology
Commercially available	Yes	Yes	Yes	No ( <i>in vivo</i> ), Yes ( <i>in vitro</i> )

1PEM, one-photon excitation microscopy; 2PEM, two-photon excitation microscopy; 3DEM, 3-dimension electron microscopy; CLEM, correlative light and electron microscopy; DSLIM, digitally scanned light-sheet microscopy; LSFM, light-sheet fluorescence microscopy; PALM, photo-activated localization microscopy; ROI, region of interest; SIM, structured illumination microscopy; SPIM, single plane illumination microscopy; STED, stimulated emission depletion; STORM, stochastic optical reconstruction microscopy; ZF, zebrafish.

sample is scanned by a laser spot, i.e. confocal laser scanning microscopy (CLSM) (Fig. 1A). The emitted light from the focal plane is selected through a pinhole and optically conjugated with the focal plane before being detected on sensitive photodetectors. Although this technology has provided a tremendous amount of biological insights, it was limited by its acquisition speed, which was not sufficiently fast to capture dynamic subcellular events. Acquisition speed has recently been improved by the coupled development of resonant scanners and sensitive detectors. Accelerated acquisition regimes can also be achieved by using spinning disk confocal microscopy (SDCM). Instead of scanning the sample point-by-point, SDCM is capable of acquiring multiple points at the same time (Fig. 1A), on a charge-coupled device (CCD) camera, thus increasing the data acquisition rate. The main drawback of SDCM is the cross-talk between pinholes; this can be circumvented by increasing the inter-pinhole distance or by decreasing the out-of-focus light by using two-photon excitation

(Shimozawa et al., 2013). Both CLSM and SDCM have been ground-breaking for imaging *in vitro* as well as *in vivo*; for instance, relatively thin model systems (Fig. 1C), such as tissue explants and organoids, or small organisms, such as *Caenorhabditis elegans* (Nguyen et al., 2016) or zebrafish embryos (Kissa and Herbomel, 2010). Recent advances in CLSM have led to the development of the so-called Airyscan concept (Zeiss), whose detector array allows to efficiently collect the photons from the entire Airy diffraction image with confocal resolution owing to the intrinsic size of each detector. Thus, when coupled to ultra-sensitive detectors, Airyscan exploits an increase in photon yield to improve sensitivity, speed or resolution (<http://blogs.zeiss.com/microscopy/news/en/zeiss-lsm-880-airyscan-introducing-fast-acquisition-mode/>).

CLSM has been successfully used for imaging microcirculation in the rat brain (Villringer et al., 1994) and astrocytes in the mouse brain (Pérez-Alvarez et al., 2013). SDCM has been used to describe the recruitment of platelets in several mouse organs, including brain,

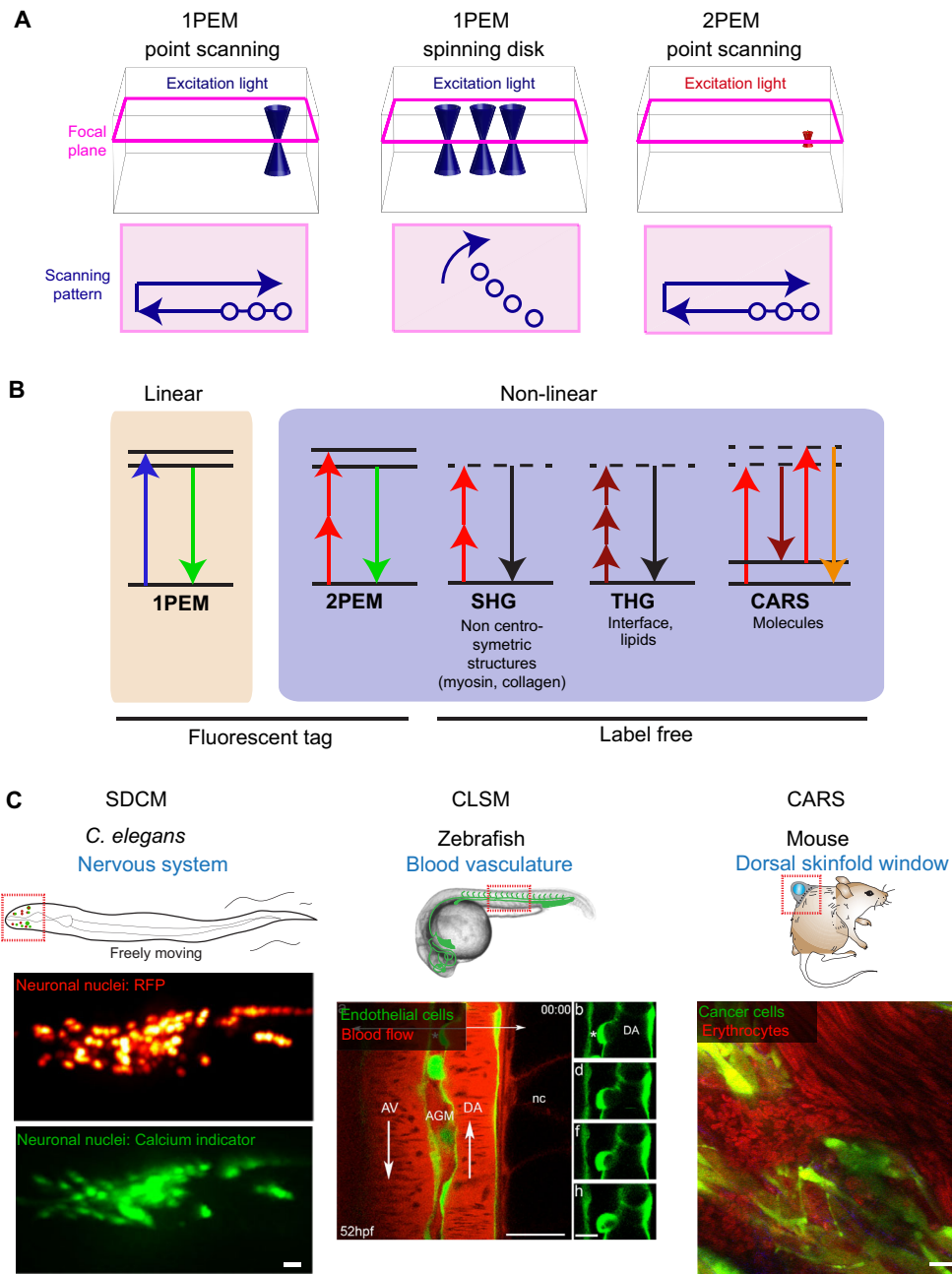


**Fig. 1. Technical considerations and biological applications of intravital imaging.** (A) Comparison between one-photon excitation microscopy (1PEM) and two-photon excitation microscopy (2PEM). In 1PEM, the excitation light illuminates the focus (pink line) and out-of-focus planes, and a pinhole is needed to eliminate the signal originating from the out-of-focus planes. In 2PEM, excitation occurs only at the focus plane (pink line) and a pinhole is not required because the excitation is already confocal. As shown in the illustrations at the bottom, 1PEM and 2PEM point scanning create the image of the sample by imaging one point at a time, whereas the spinning disk performs multiple acquisitions simultaneously. (B) Jablonski diagram of linear and nonlinear processes. 1PEM: the molecule is excited by absorbing a photon; after internal conversion the molecule returns to its ground state and emits a red-shifted photon. 2PEM: the molecule is excited by absorbing two photons at the same time; it returns to the ground state by emitting one photon of energy that is higher than that of the excitation photons. Second harmonic generation (SHG): two photons are scattered by a molecule and emit one photon of half the excitation wavelength. Third harmonic generation (THG): three photons are scattered by a molecule and produce one photon of a third of the excitation wavelength. Coherent anti-stokes Raman spectroscopy (CARS): a pump photon (first red arrow, pointing up) excites the molecule to a virtual state before a second photon (referred to as Stokes photon; brown arrow pointing down), forces the de-excitation of the molecule to above ground state. A third photon from the pump beam (second red arrow, pointing up) is used to elevate the molecule to a new virtual state, from which it will relax and emit a blue-shifted photon (orange arrow pointing down). (C) Biological applications of linear and nonlinear microscopy processes. Left: spinning disk confocal microscopy (SDCM) is used for ultra-fast neuronal calcium imaging in a freely moving *C. elegans*. (Red: neuronal nuclei; green: the protein calcium sensor GCaMP6s). Scale bar: 10  $\mu$ m. Adapted with permission from Nguyen et al., 2016. Middle: confocal laser scanning microscope (CLSM) used for long-term (>70 h) time-lapse imaging of zebrafish vasculature, highlighting the emergence of a hematopoietic stem cell in the ventral wall of the dorsal aorta (green). Scale bars: 25  $\mu$ m (left panel), 10  $\mu$ m (right panel). Adapted with permission from Kissa and Herbomel, 2010. Right: multimodal nonlinear microscopy used to study tumor mass and vascularization within a skinfold dorsal chamber in mouse. Red, erythrocytes imaged by using CARS; green, cancer cells imaged by using 2PEM. Scale bar: 15  $\mu$ m. Adapted with permission from Lee et al., 2015.

liver and cremaster muscle (Jenne et al., 2011). Nevertheless, most of the visible light is absorbed (Boulnois, 1986) and scattered by tissues, thus limiting depth in intravital confocal microscopy to the organ surface of an animal (<100  $\mu\text{m}$  in thickness) (Masedunskas et al., 2012; see also Fig. 1C). In order to be able to image relevant biological events deeper in tissues, researchers took advantage of the optical transparency of the tissues in the near-infrared or infrared wavelengths (Boulnois, 1986) and of the discovery of pulsed lasers to develop two-photon microscopy (Helmchen and Denk, 2005), thereby making it possible to image deeper into the tissues of living animals.

### Multiphoton microscopy for imaging *in vivo*

The principle of two-photon absorption was originally described in 1931 (Göppert-Mayer, 1931) but it took until 1963 for the first pulsed laser to be developed (Peticolas et al., 1963); later on, this turned into the first two-photon laser scanning microscope (Denk et al., 1990). In classic CLSM, the energy carried by a single laser photon allows the excitation of fluorophores, whereas in two-photon excitation microscopy (2PEM), each photon carries half the energy and, thus, the excitation requires the simultaneous absorption of two photons (Fig. 1B). For this purpose, the photon density has to be high, both in time (femtosecond laser pulses) and in space (through the usage of lenses with high numerical aperture). Compared to classic CLSM, 2PEM can achieve non-invasive, deep imaging in voluminous live samples owing to several properties. First, the nonlinear properties of the multiphoton absorption confine the excitation to a small volume (Fig. 1A), resulting in an enhanced signal-to-background-noise ratio and a lesser phototoxicity (Helmchen and Denk, 2005). Second, infrared light is less well absorbed and scattered by biological tissues, and allows deeper imaging than when regular one-photon excitation (1PEM) microscopy (hereafter referred to as 1PEM) is applied. Because the excitation is limited to the focal plane, the photo-toxicity typically induced by 1PEM is drastically reduced. Pinholes are not required in two-photon excitation (2PE) microscopy (hereafter referred to as 2PEM), which makes it possible to use non-descanned detectors that can be placed closer to the sample, thereby enhancing the signal. Together, these advantages allow imaging of biological phenomena that take place deep within a living organism. For example, 2PEM can easily image through the skin of living mice, and has been used for tracking xenografted cancer cells and their immune responses in mouse ear skin (Li et al., 2012), and for tracking features of muscle diseases in neuromuscular junctions (Mercier et al., 2016). Skin pigmentation can be – owing to light absorption – a major barrier in optimized imaging, and imaging windows have been developed for rodents to reach the deeper organs. This technique has been particularly useful in cancer biology for the imaging of subcutaneous tumors (using the dorsal skin-fold chamber), lungs (Headley et al., 2016), brain (Kienast et al., 2010) and abdominal organs, such as the intestine (Ritsma et al., 2014) or the liver (Ritsma et al., 2012), as well as mammary tumors (Zomer et al., 2015). Although regular 2PEM allows penetration of up to 1 mm into tissues (Theer et al., 2003), improved imaging depths through scattering tissues (the heterogeneity of biological tissues leads to photon absorption and re-direction, without any loss in energy, that can create imaging artifacts) can be obtained by increasing the wavelength of excitation to >1000 nm with optical parametric oscillators (Kobat et al., 2011). Furthermore, the use of powerful pulsed femtosecond lasers opened the door to nonlinear microscopy, which has the unique ability to provide endogenous signals from living non-labeled scattering tissues (discussed below).

### Label-free intravital imaging

The most-commonly used techniques to perform intravital imaging require the presence of fluorescently labeled molecules and, therefore, do not allow the imaging of endogenous non-labeled structures and their physiological environment. Below, we discuss several nonlinear microscopy methods that exploit the physical and optical properties of molecules, as well as advanced optics, for the imaging of non-labeled material within living tissues.

Second harmonic generation microscopy (SHG) (Fig. 1B) is the most popular nonlinear imaging technique and has first been described in 1963 (Franken et al., 1961). SHG allows to visualize endogenous, non-centrosymmetric molecules, such as collagen and myosin, which upon light scattering produce a photon at half the incident wavelength. SHG has been proven to be a highly useful technology for the non-invasive intravital imaging of the collagen-rich microenvironment during tumor invasion (Wang et al., 2002), of muscle defects in the mouse ear (Mercier et al., 2016) and of zebrafish embryos (Ramsbacher et al., 2015). Furthermore, nanoparticles generating second harmonics have been used *in vivo* and represent new imaging tools (Grange et al., 2011; Pantazis et al., 2010).

Third harmonic generation (THG) microscopy (Fig. 1B) is a non-linear scattering process that originates from the polarization properties of the excited volume and from variations of the refraction index in that volume, such as in water–lipid and water–protein interfaces found, for instance, in cellular membranes and extracellular matrix structures (Weigelin et al., 2016). THG is mostly used in tumor biology to visualize ECM structures (Alexander et al., 2013) but has also been used to image lipid bodies in *Drosophila melanogaster* embryos (Débarre et al., 2006). Another label-free imaging approach relies on the Raman effect (also known as Raman scattering), i.e. the inelastic scattering of a photon upon interaction with matter, which has first been described in 1928 by Raman and Krishnan, 1928. Coherent anti-Stokes Raman scattering (CARS) microscopy detects structures by simultaneously illuminating a sample with a pump and a Stokes beam, upon which a pump and a Stokes photon match the energy of the excited vibrational state of a molecule within the sample. A second pump photon is used to elevate the molecule to another virtual state before relaxation of the molecule causes an emission of photons (anti-Stokes emission) that is shifted into the blue spectrum (Fig. 1B). Intravital CARS microscopy has been applied to *C. elegans* to examine the impact of genetic variations in metabolic pathways on lipid storage (Hellerer et al., 2007) (Fig. 1C). One of the great advantages of using nonlinear microscopy *in vivo* is the possibility of combining fluorescent signals with information obtained from endogenous, unlabeled structures. For example, SHG and CARS have been combined with 2PEM in the imaging of tumors within dorsal skin-fold chambers, and have provided access to tissue structures (SHG), cancer cell behavior (2PEM) and blood flow measurement (CARS) *in vivo* (Lee et al., 2015).

Yet, although the field of intravital imaging in higher organisms has expanded tremendously in the past few years, this approach, nevertheless, suffers from drawbacks associated with light absorption and scattering that impair its use for high-resolution imaging of subcellular events of interest. These limitations can be circumvented by using the CLEM approaches we discuss in the last section of this review. However, imaging of less voluminous samples or organisms can be performed with several approaches described in the following sections.

### Light-sheet fluorescence microscopy (LSFM)

An important concern in modern cell biology is the ability to perform observations over long periods of time to follow, for example, processes during embryonic development. This can now be achieved by using light-sheet fluorescence microscopy (LSFM). LSFM was originally developed to overcome the resolution limitations of conventional fluorescence microscopy, in which the resolution is diffraction limited, with the axial resolution being about twice that of the lateral resolution. LSFM is an optical imaging technique, initially based on a plane excitation that is obtained by focusing a laser beam through a cylindrical lens, while the detection is performed in an orthogonal plane (Reynaud et al., 2008). This optical geometry retains the same diffraction resolution limitation in the detection plane but offers the same resolution in the excitation axis. Nowadays, complementary metal oxide semiconductor (cMOS) cameras are used to ensure a detection of the entire field at high speed and high resolution, way beyond the detection obtained with scanning technologies. Thus, owing to a reduced acquisition time as well as the simultaneous and selective illumination of the detection plane, LSFM significantly decreases the phototoxicity and photobleaching compared to classic confocal microscopy (Keller and Ahrens, 2015; Lim et al., 2014; Pampaloni et al., 2015; Weber and Huisken, 2011); it is therefore highly useful in imaging dynamic events that take place in small and transparent organisms and embryos. In this section, we briefly focus on the two main technological strategies that have been developed to achieve this specific illumination, single plane illumination microscopy (SPIM) and digitally scanned light-sheet microscopy (DSLM). We also provide a snapshot of their current use by describing some of the biological insights that LSFM have made possible.

#### Single plane illumination microscopy (SPIM)

Single plane illumination microscopy (SPIM) is the first version of LSFM; here, a cylindrical lens focusing light orthogonally to the observation plane creates the light sheet (Fig. 2A). This technology is suitable for imaging of entire animals and was highlighted already in 2004 as a means to image deep inside living zebrafish and *Drosophila* embryos. Indeed, LSFM turned out to be highly efficient in following morphogenetic events for several hours at high resolution, high speed and without photo-damaging the embryos (Huisken et al., 2004). LSFM has since continuously evolved, resulting in the development of optical systems that use several illumination and detection paths, such as multiview (MuVi)-SPIM (Krzic et al., 2012) or SimView SPIM (Tomer et al., 2012). These techniques are based on a dual light-sheet system that can switch between four different light pathways in less than 50 ms. This setup allows the acquisition of four, nearly simultaneous images from different regions in the sample (scanned in one dimension by using a piezo stage), thus making it possible to image a large-volume sample for instance a *Drosophila* embryo in 35 s (Tomer et al., 2012) (Fig. 2B). Alternatively, if the acquisition rate is not limiting, LSFM can be coupled to a sample holder mounted on a rotational stage (Jakob et al., 2016).

The potential of SPIM for high-speed *in vivo* imaging has been elegantly demonstrated for the developing Zebrafish heart – this being a very challenging task owing to its small size (250  $\mu\text{m}$ ) and its high beat frequency of 2–4 Hz (Mickoleit et al., 2014). Subsequently, multi-view SPIM strategy (named here ‘IsoView’) was successfully used to study the development of the *Drosophila* embryo and the brain of Zebrafish larvae, with an unprecedented spatio-temporal resolution (Fig. 2C). Here, the authors compared

their setup with lattice light-sheet microscopy (see below) to emphasize the superior imaging depth and acquisition speed their particular approach can afford (Chhetri et al., 2015). In addition, SPIM has been combined with laser ablation (optical damaging of cells or intracellular region by using a powerful and focused laser) to unravel mechanical coupling of two important morphogenetic events in *Drosophila*: endoderm invagination and axis extension (Lye et al., 2015). In addition, several groups have implemented SPIM to accelerate commonly performed imaging. For example, MuVi-SPIM together with a customized software package can be used to increase acquisition speed and analysis by several orders of magnitude, which allows to – almost instantaneously – record individual cell shapes over an entire embryo (Stegmaier et al., 2016).

#### Digitally scanned light-sheet microscopy (DSLM)

In DSLM, the illumination plane is obtained by deflecting the beam with a galvanometric mirror through the excitation objective (Fig. 2D). Here, 3D volumes are obtained by 2D scanning methods. This method was pioneered by the Stelzer group in 2008 and has been applied for imaging the early stages of development of zebrafish embryos (Keller et al., 2008). In this study, the authors successfully reconstructed in 3D the collective migration patterns of several cell type precursors during gastrulation with an unprecedented temporal and  $x/y$  resolution. When combined with Bessel beams and/or multiphoton illumination, an increase in spatial resolution can be obtained. Bessel beam illumination is an alternative method to the typical Gaussian beam illumination and consists of feeding back the focal plane of the excitation objective with an annular illumination (Planchon et al., 2011). However, Bessel illumination creates side lobes (i.e. lateral intensity peaks) in the illumination plane, which impair reaching the desired resolution. Therefore, in addition to the Bessel illumination, it is currently possible to use diffractive optics that generate a structured illumination convoluted to the Bessel beam (Gustafsson et al., 2008); this allows image acquisition below the diffraction limit (Gao et al., 2012). Moreover, this setup strongly benefits from a two-photon illumination with associated increased penetration and decreased photobleaching and/or phototoxicity (Truong et al., 2011); this drastically reduces the risk of adversely affecting the physiology of the event studied (Ahrens et al., 2013; Wolf et al., 2015). A recent, but main update in this field was provided by the group of Eric Betzig with the demonstration of the lattice light-sheet microscopy (Chen et al., 2014) as an improvement of Bessel beam LSFM. In this setup, a fast-switching, spatial light modulator is used to generate the Bessel beam mask before it enters in the excitation objective. This permits a tremendous gain of speed at a resolution that is equivalent to that obtained with SIM (Chen et al., 2014; see below). More recently, by using the same strategy of coupling super-resolution and LSFM, lattice light-sheet–point accumulation for imaging of nanoscale topography (PAINT) microscopy has been introduced (Fig. 2E). Although image acquisition may take several days, this technique makes it possible to extend the 3D visualization of single-molecule localizations in thicker and more voluminous samples, such as in dividing cells (Legant et al., 2016).

At the moment, there are only few examples for biological applications of the latest versions of DSLM. For example, lattice light-sheet microscopy has been used to study the microtubule organization during HeLa cell division *in vitro* (Yamashita et al., 2015). Owing to the superior temporal and spatial resolution that can be achieved (below the diffraction limit and with a time interval of <1 s), the authors provided new insights into the growth

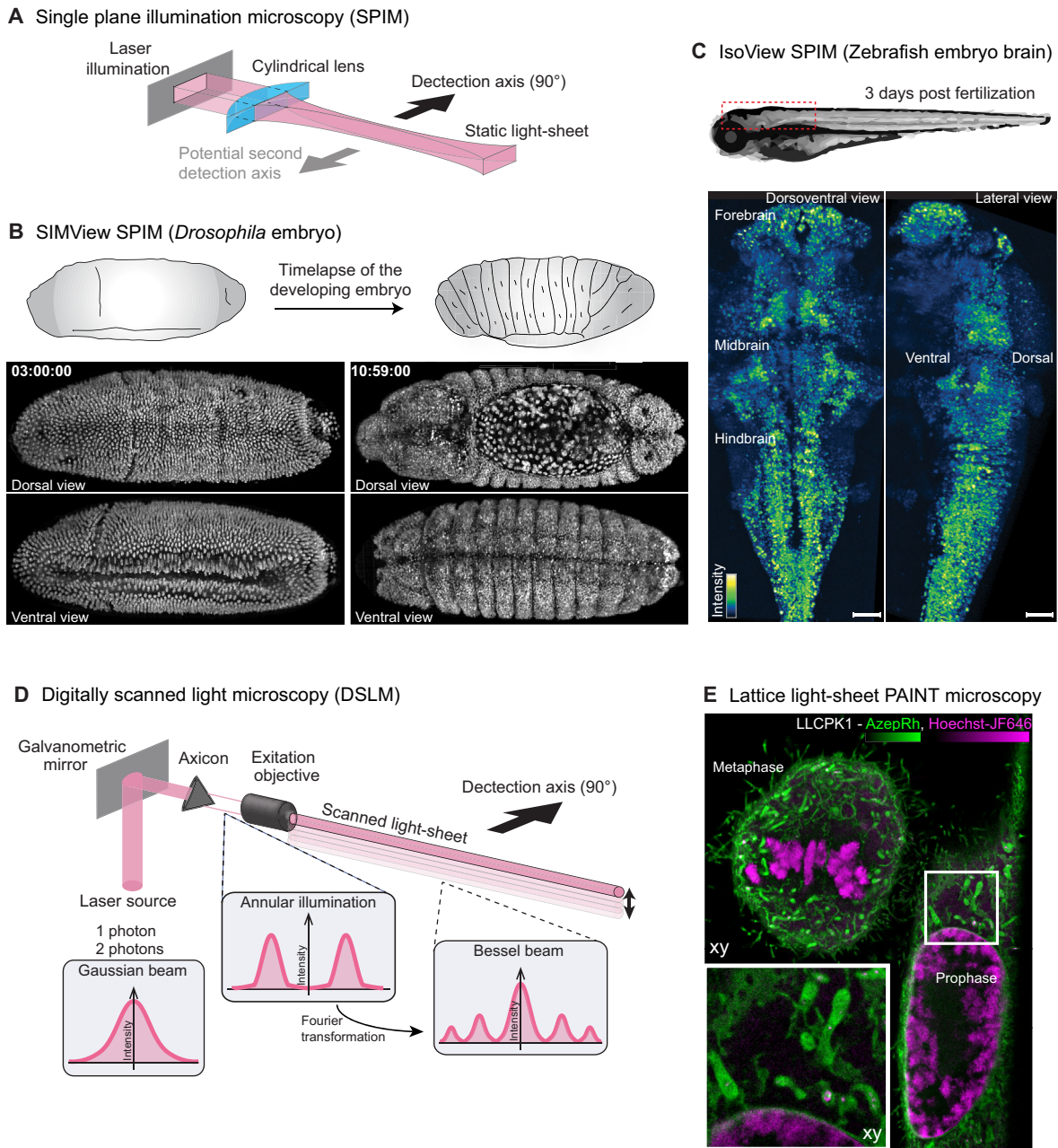


**Fig. 2. Light-sheet microscopy and examples of biological applications.** (A) Optics setup for SPIM. A cylindrical lens induces the formation of the light-sheet that can be scanned in 1D for volumetric imaging. Arrows indicate the detection axes (black arrow, usual 90° detection axis; gray arrow, potential second objective position for multiview SPIM). (B) SIMView SPIM imaging of nuclei during the development of *Drosophila* embryo, illustrating the possibility to carry out long-term image acquisition without photo-damage or photobleaching; adapted with permission from Tomer et al., 2012. (C) IsoView SPIM of zebrafish embryo brain (using a nuclear GCaMP6  $\text{Ca}^{2+}$  probe), illustrating the power of this technique to record volumetric data *in vivo* at high speed and high resolution. Scale bars: 50  $\mu\text{m}$ . Adapted with permission from Chhetri et al., 2015. (D) Illustration of the optical setup for Bessel beam digitally scanned light microscopy (DSLM), for which the beam is scanned in 2D for imaging in three dimensions. Laser source can be either one or two photons. The insets show the evolution of the laser intensity profile (Gaussian beam) through the axicon (a type of lens with a conical surface), leading to annular illumination, as well as the beam profile after being focused through the excitation objective. The Bessel profile is created at that step. (E) Imaging of dividing porcine kidney cells by using PAINT DSLM. DNA is labeled with Hoechst-JF<sub>646</sub>, intracellular membranes are labeled with Azeprh. At cost of acquisition speed and a complex post-processing procedure, this technology allows so-far-unprecedented 3D resolution of a wide field of view. Adapted with permission from Legat et al., 2016.

mechanisms of microtubules. In addition, by imaging living zebrafish embryos with LFSM, the interaction between Schwann cells and axons during neuron damage repair was observed *in vivo* (Xiao et al., 2015). More recently, two-photon Bessel beam light-sheet microscopy was optimized to study how cells

maintained in a 3D culture mechanically react to changes in their microenvironment, at a subcellular level and without spatial constraint (Welf et al., 2016). Taken together, these recent studies demonstrate that LFSM is a particularly promising tool for studying mechano- and cell biology.

### Requirements for LSFM

It is important to emphasize here that LSFM is extremely demanding with regard to computing resources owing to the large datasets that need to be handled. Image acquisition generates hundreds of gigabytes that need to be stored quickly. Thereafter, post-processing and reconstructions in three dimensions require enormous computer resources. These computing demands need to be consciously addressed in the future to ensure LSFM is amenable to cell biologists. In addition, only few commercial systems that are available for the wider scientific community currently exist for LSFM. This is mainly due to the fact that optical setups are typically designed and mounted in order to address a specific biological question of interest.

Taken together, there is, however, no doubt that LSFM will be used more widely in the coming decade. Thanks to its versatility, it offers multiple advances over other imaging approaches, such as increased spatio-temporal resolution with significantly reduced phototoxicity and/or photobleaching at all scales (Fig. 2B,C and E; Table 1), from *in toto* imaging of small animals with SPIM, to studying subcellular compartments in detail with DSLM.

### Super-resolution microscopy – digging below the light-diffraction

Fluorescence microscopy has become one of the most useful tools for cell biologists owing to its non-invasive properties and high versatility. The past decades have witnessed significant technological improvements of microscopy setups regarding sensitivity and acquisition speed, as well as the development of brighter and more photostable fluorescent probes. These developments shifted fluorescence microscopy – which was mainly used for descriptive purposes – towards a more quantitative approach, in which the careful analysis of the large datasets allowed the deciphering of complex cellular processes at the biological and physical level. However, conventional fluorescence imaging is limited by light diffraction to a resolution (i.e. the minimal distance at which two physically distinct objects will appear as separated) of ~200 nm in the *x/y* plane (lateral resolution) and ~600 nm along the *z* axis (axial resolution), which is several orders of magnitude above the size of single proteins. Thus, reaching a resolution of a few tens of nanometers had been a main quest for microscopy optics experts and imaging computer scientists, and ultimately led to the 2014 Nobel Prize being awarded to Eric Betzig, Stefan Hell and William Moerner for their essential contributions in the development of super-resolution microscopy or nanoscopy. Furthermore, since 2007 the introduction of commercially available systems has granted the cell biology community access to these new tools, opening the door to a new era of cellular and sub-cellular imaging. Because subcellular and biomechanical processes are fast, dynamic and reversible in nature, they require fast imaging techniques to be monitored (Eyckmans et al., 2011; Hoffman et al., 2011; Janmey and Miller, 2011). Thus, we will introduce here nanoscopy approaches that can be used to study subcellular and biomechanical mechanisms by describing selected examples.

#### Stimulated emission depletion (STED) microscopy

An important quest for cell biologists is to have access to live and high-resolution imaging of their favorite fluorescent proteins or molecules. This can now be performed by using stimulated emission depletion (STED), which facilitates, for example, live intracellular vesicular trafficking in multiple situations. STED microscopy works on the basis of a scanning confocal microscope,

where resolution is improved by using a doughnut-shaped depletion beam that is shifted into the red-light spectrum, which ‘wraps’ the excitation beam (Fig. 3A). In this configuration, fluorophores illuminated by the depletion beam are forced to return to ground state and emit at depletion wavelength, which is filtered out, while the ‘nondepleted’ fluorophores at the center, emit normally. This optical trick results in a smaller emission volume and increases the lateral resolution to 20–70 nm (Klar et al., 2000; Willig et al., 2007). When live imaging is desired, speed acquisition may be reduced by relying on higher laser output. However, increased laser power will ultimately lead to increased phototoxicity. The use of continuous wave (CW) beams and time-gated detection allows the effective use of reduced laser powers and efficient increased resolution, thereby making gated CW STED compatible with live imaging (Willig et al., 2007; Westphal et al., 2008; Vicidomini et al., 2011).

STED was effectively used to monitor vesicular trafficking in real-time in living cultured neurons (Westphal et al., 2008), image GFP-labeled neurons in *Caenorhabditis elegans* (Rankin et al., 2011) and, more recently, follow the trafficking of EGFP-labeled vesicles in living neurons in *Drosophila* larvae with a rate above 100 frames per second (Schneider et al., 2015). These examples suggest that STED microscopy is well suited to image fast and dynamic processes in small transparent organisms, such as *C. elegans*, *Drosophila melanogaster* or zebrafish embryos. However, when considering higher organisms, conventional lasers are not able to perform intravital imaging, and confocal microscopes must be coupled to selective plane illumination microscopy (SPIM) or multiphoton excitation (discussed above). For instance, a combination of STED and SPIM was used to image >100  $\mu\text{m}$  deep into the tissues of entire zebrafish embryos, resulting in a 40–250% improvement of resolution (Friedrich et al., 2011; Scheul et al., 2014; Friedrich and Harms, 2015). Axial resolution, which is often a limiting factor when using light-sheet illumination, has recently been significantly improved with reversible saturable or switchable optical linear fluorescence transitions (RESOLFT) nanoscopy and, thus, offers access to high-speed imaging with lowered laser power (Hoyer et al., 2016). 2PE lasers have a better penetrance into the tissue (<1 mm) and reduced photo-damaging, and the resulting laser spot is spread less along the *z* axis, thus providing a better axial resolution (Denk et al., 1990; Helmchen and Denk, 2005). 2PE-STED allowed, for example, to monitor, in real-time, the dynamics of neurons within the brain of living mice through a cranial window (Fig. 3D) to a depth of 15–90  $\mu\text{m}$  and with a resolution of ~40–90 nm (Berning et al., 2012; Takasaki et al., 2013; Willig et al., 2014; Coto Hernández et al., 2016). The major technical challenge is based on the fact that efficient STED requires a perfect alignment of the excitation and depletion beams. However, as tissues are not homogenous, imaging of deeper layers unavoidably decreases resolution (Takasaki et al., 2013).

#### Structured illumination microscopy (SIM)

Although image reconstruction remains very complex and artifact-prone, structured illumination microscopy (SIM) is the simplest of the super-resolution techniques. It works in the basis of a wide-field microscope into which a grating pattern is inserted into the light path. By generating interferences (i.e. *Moiré* fringes), SIM provides access to spatial information regarding the fluorescence signal. The pattern is rotated at predefined angles, and several images are acquired, usually nine to 15 (Fig. 3B). The spatial information revealed by each frame is then computed to reconstruct a sub-diffraction image, which allows to double the resolution compared



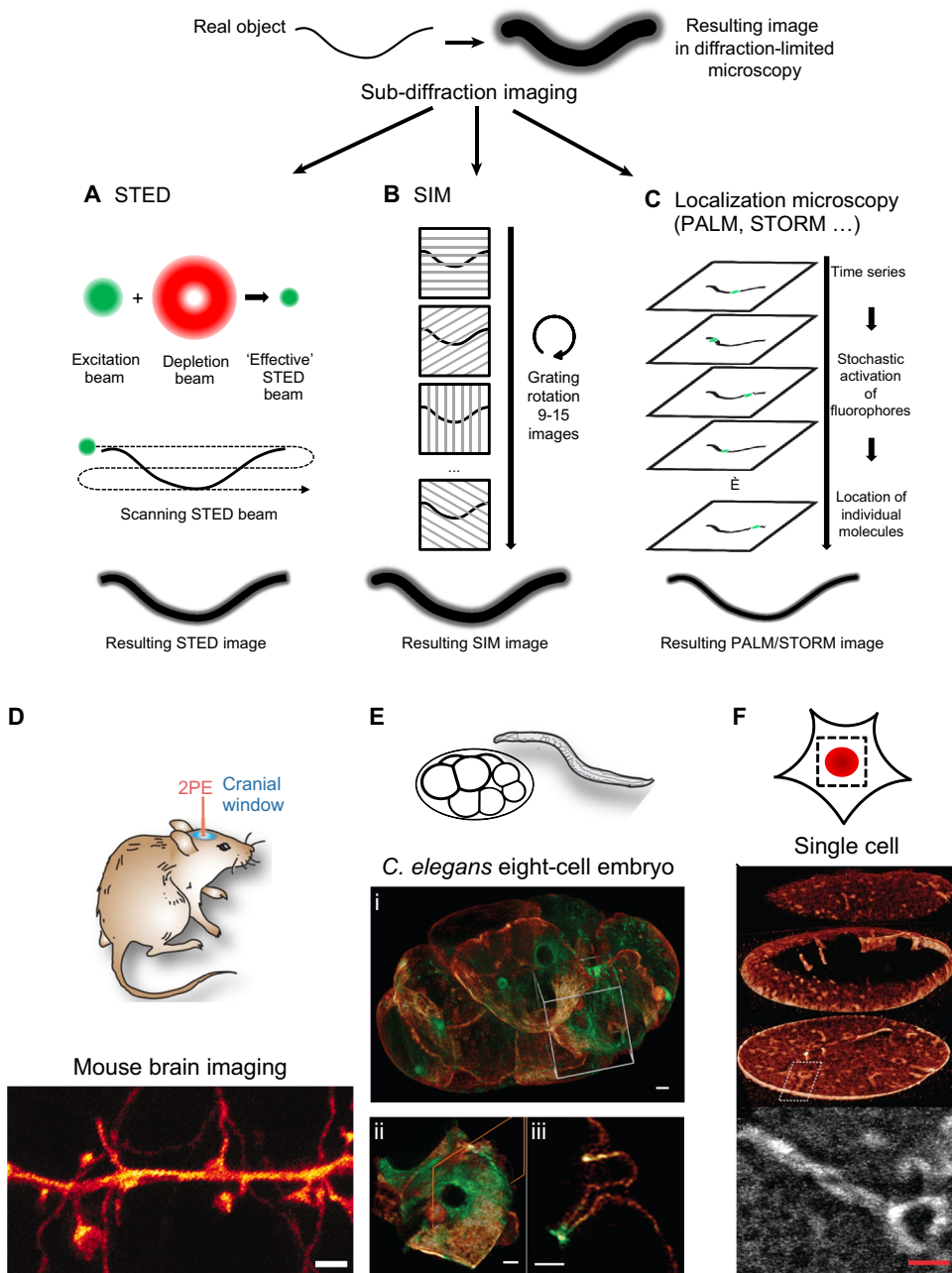


**Fig. 3. Super-resolution microscopy and its biological applications.** (A) Stimulated emission depletion (STED) microscopy is achieved on the basis of a line-scanning confocal microscope, in which the resolution is increased by using a second red-shifted depletion beam that 'depletes' unwanted activated fluorophores at the edges of the diffracted excitation beam. This results in a detection size in the focal plane reduced to the tens of nanometers. (B) Structured illumination microscopy (SIM) microscopy is a widefield microscopy technique. Here, increased resolution is achieved by introducing a diffraction grating in the optical path. The grating is then turned to selected angles and the sub-diffraction image is reconstructed from all the images acquired (typically 9 to 15). (C) Localization microscopy techniques, such as PALM and STORM, achieve high resolution by excitation of stochastic fluorophores coupled with computer-assisted high-precision localization of individual molecules. (D) Direct STED imaging of live mouse brain through an observation window at a depth of 10–15  $\mu\text{m}$ . 2PE, two-photon excitation. Adapted with permission from Berning et al., 2012. Scale bar: 1  $\mu\text{m}$ . (E) *C. elegans* eight-cell embryo expressing GFP-myosin and mCherry-membrane marker. (i) Live image using SIM combined with Bessel beam illumination. (ii) Cropped view from the 3D section in i. (iii) Single-plane view corresponding to the orange plane in ii, showing a cytokinetic ring. Adapted with permission from Gao et al., 2012. Scale bar: 2  $\mu\text{m}$ . (F) 3D rendering of the nuclear envelope of U2OS cell expressing Dendra2–LaminA excited with dithered lattice light-sheet illumination and acquired with 3D PALM (top). Super-resolution maximum-intensity projection of the boxed area (bottom). Adapted with permission from Chen et al., 2014. Scale bar: 1  $\mu\text{m}$ .

to conventional microscopy (Gustafsson, 2000). Alternatively, to protect living samples from excessive light exposure, the nonlinearity of photo-convertible fluorescent proteins can be used with SIM to achieve a similar resolution (Rego et al., 2012; Li et al., 2015). Furthermore, by engineering the grating to create three coherent beams, which form an illumination pattern varying laterally and axially or by using multifocal illumination patterns, the resolution can also be improved by a factor of two in all directions (Gustafsson et al., 2008; York et al., 2012).

Since SIM works on the basis of wide-field imaging and thus requires only a few planes to reconstruct a sub-diffraction image, it is probably the best-suited live-imaging approach to monitor dynamic events at subcellular level. However, one should keep in mind that resolving structures of <50–100 nm in size remains a difficult task. Nevertheless, SIM was successfully used to monitor

the dynamics of subcellular structures and organelles, such as mitochondria, clathrin-coated vesicles, microtubules and actin cytoskeleton in living cells, both in 2D and 3D at a speed of up to 11 frames per second (Fiolka et al., 2012; Kner et al., 2009; Shao et al., 2011). More recently, up to 200 frames were obtained in <0.5 s by using total internal reflexion fluorescence (TIRF) with a high numerical aperture objective in order to limit out-of-focus excitation and to increase the axial resolution on the basal side of the sample (Li et al., 2015). The use of cMOS cameras, which are faster than regular electron multiplying CCD (EMCCD) cameras, helps to further improve the number of frames acquired per second and allows the 3D recording of the entire volume of a single cell in culture within ~1 s (Fiolka et al., 2012). Recently, 3D-SIM has been combined with lattice light-sheet illumination and achieved a similar rate of acquisition with less invasive light exposure (Li et al.,

2015). Furthermore, the combination of SIM and Bessel beam plane illumination was used to image the development of a *C. elegans* embryo (Fig. 3E), and the chromosomal rearrangement in a *Drosophila* syncytium with a three- to fivefold increase in resolution and an image acquisition speed that captured the total volume of the embryo within 1 s (Gao et al., 2012). Furthermore, multifocal plane illumination SIM was used to image the dynamics of the endoplasmic reticulum in cultured cells at 100 frames per second, or of the blood flow in zebrafish at 37 frames per second (York et al., 2013).

### Localization microscopy

Localization microscopy encompasses a family of techniques that allows the precise localization of fluorophores at single-molecule level; here, the precision directly reflects the number of photons emitted by a single source. The sub-diffraction image is then reconstructed from the localizations obtained for the single fluorophores. These techniques rely on the possibility to excite only a few fluorophores within the image plane, rather than all of them; this makes it possible to differentiate between fluorophores, whose distance is below the diffraction limit. This is achieved by photo-manipulation of fluorophores, i.e. by turning them on or off (Fig. 3C). In photo-activated localization microscopy (PALM), photo-manipulation is mediated by using photo-activatable fluorescent proteins (Betzig et al., 2006; Hess et al., 2006), whereas stochastic optical localization microscopy (STORM) uses a pair of organic dyes, of which one - following Förster resonance energy transfer (FRET) - activates the second one, which is imaged until it is switched off (Heinlein et al., 2005; Rust et al., 2006). Furthermore, direct STORM (dSTORM) allows the localization of single molecules by photoswitching an organic dye between its fluorescent and non-fluorescent state (Heilemann et al., 2005, 2008). Altogether, localization microscopy is the most efficient sub-diffraction technique with a lateral resolution  $<10\sim 20$  nm (Betzig et al., 2006; Hess et al., 2006). Localization microscopy has also been implemented for 3D imaging, and several technical approaches have been used to achieve sub-diffraction 3D imaging. For instance, in combination with PALM, simultaneous detection of each imaged focal plane and of a second plane that is 350 nm closer to the objective, improves the axial resolution to 75 nm (Juetz et al., 2008). In addition, combination of multifocal excitation and localization microscopy has demonstrated the simultaneous imaging of a 4- $\mu\text{m}$  volume within single cells with a resolution of  $20\times 20\times 50$  nm (Hajj et al., 2014).

The main drawback of localization microscopy is that the sub-diffraction resolution is achieved by localizing single fluorophores over time, which makes it less suitable for imaging fast dynamic processes. However, localization microscopy can be used for high-resolution single-particle tracking (spt) (Manley et al., 2008), which can be very useful for understanding key cell biological events. For example, spt-PALM has recently been applied to track integrins within and outside of focal adhesions, and to quantify their diffusive properties (Rossier et al., 2012). Furthermore, this approach was used to demonstrate that the mechanical properties of the glycocalyx layer promote focal adhesion growth by channeling membrane-associated integrins into clusters (Paszek et al., 2014). In another example, 3D PALM was used in *Drosophila* embryos to analyze the clustering of E-cadherin at cell–cell junctions (Truong Quang et al., 2013). In addition, PALM has been combined with confocal correlation microscopy for high-resolution mapping of glutamate receptors in individual neurons that had been annotated by standard confocal microscopy in *C.*

*elegans* (Vangindertael et al., 2015). As live imaging also requires imaging at high speeds in order to be able to track dynamic events, faster CMOS cameras have been developed that allow the recording of fast events at high-resolution (Huang et al., 2013). Moreover, 3D PALM has recently been combined with lattice light-sheet illumination to image single cells in culture (Fig. 3F), as well as mouse stem cells spheroids at high speed (Chen et al., 2014). Taken together, although super-resolution imaging offers new possibilities in live and *in vivo* cell biology, there are still some limitations that impede obtaining nanoscale resolution of these events (Table 1).

### Correlative light and electron microscopy (CLEM) – moving towards nanoscale resolution of dynamic *in vivo* phenomena

The most interesting biological events usually occur only infrequently and involve single molecules or organelles that are separated by only few nanometers. The perfect imaging approach, thus, would make it possible to obtain macroscopic views of tissues and structures and, at wish, to easily zoom into the most-discrete details or subcellular structures, organelles or proteins. As discussed above, live imaging with light microscopy is extremely useful to characterize the dynamics of cellular events *in vivo* and allows imaging of living samples in 3D, but it only has a limited spatial resolution. Electron microscopy (EM) achieves a much higher resolution but, generally, allows the imaging of fixed specimen with a limited screening ability. This makes it a challenging technique when studying rare objects such as single metastatic cells within a full organ (lung, brain, liver). CLEM combines live confocal microscopy with EM for the characterization of biological samples at high spatial and temporal resolution (de Boer et al., 2015) (Fig. 4A). CLEM can be used for virtually any biological event that can either be imaged (Goetz et al., 2014) or quantified by using biophysical approaches. The main bottleneck of the approach is the challenge to align the region of interest (ROI) that has been identified by light microscopy with the EM image. However, the increasing popularity of CLEM has led to the development of novel procedures and microscopy setups, although these were mainly developed to retrieve the ROI within a small sample, e.g. thin sections of cells or tissue to be imaged with transmission EM. The difficulty to accurately align the ROI within samples that have a complex 3D organization, such as large cells, embryos, small organisms or tissues, is still a major hurdle. Here, we will discuss the recent developments in CLEM by providing a snapshot of available procedures and techniques that help to reliably track biological events of interest at the highest spatial and temporal resolutions. We and others have recently contributed to the significant progress in the field of correlative light- and electron microscopy. By combining intravital imaging of entire organisms with EM, which we here refer to as intravital CLEM (Goetz et al., 2014, 2015; Karreman et al., 2014, 2016; Maco et al., 2013). Intravital CLEM enabled important discoveries in several areas of life science, such as cell biology (Avinioam et al., 2015), neuroscience (Allegra Mascaro et al., 2013; Maco et al., 2013), cancer research (Karreman et al., 2016), virology (Hellström et al., 2015) and developmental biology (Durdu et al., 2014; Goetz et al., 2014), and is highly likely to contribute to future breakthroughs in biological research.

### Ground-breaking *in vitro* CLEM

CLEM has primarily and successfully been applied to *in vitro* situations. By preserving the fluorescence signal within a resin-embedded block for its easy correlation with the EM image, the Briggs group has established a ground-breaking technique that

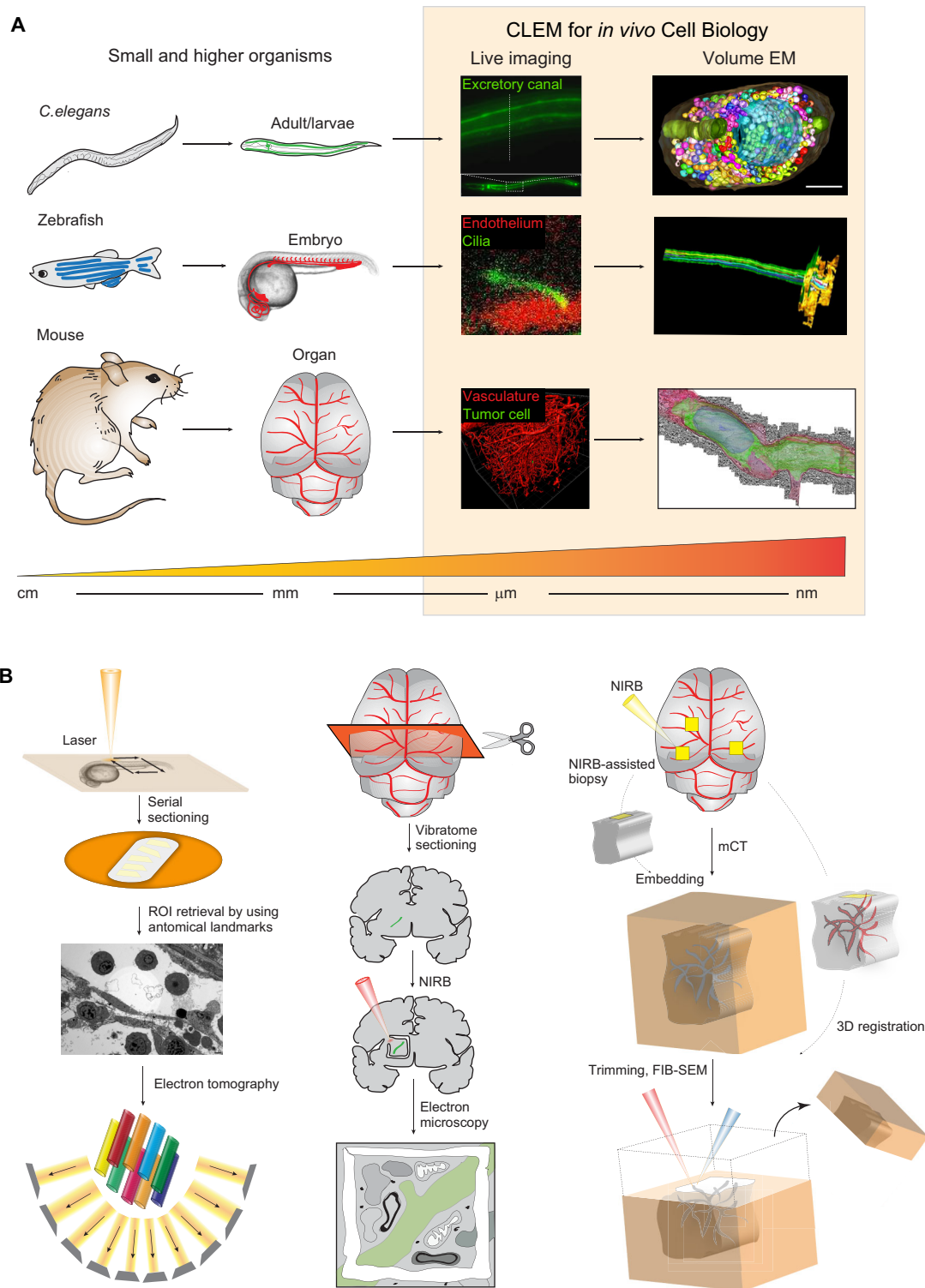


**Fig. 4. Intravital CLEM and its biological applications.** (A) Examples of intravital CLEM performed on *C. elegans*, zebrafish embryos and mice. In *C. elegans*, intravital CLEM has been used to study the ultrastructure and formation of the excretory canal by using correlative fluorescence and volume EM (serial electron tomography). Adapted with permission from Kolotuev et al., 2013. In the zebrafish embryo, CLEM was used to dissect the ultrastructure of endothelial cilia that sense and transduce blood flow forces. Adapted with permission from Goetz et al., 2014. In mice, we recently developed a multimodal approach that combines intravital 2PEM imaging, X-ray micro-computed tomography (mCT) and focused ion beam scanning EM (FIB-SEM; see panel B); this made it possible to retrieve single brain metastatic cells for their dissection at high-resolution). Adapted with permission from Karreman et al., 2016. (B) A snapshot of the existing intravital CLEM procedures. Targeted ultramicrotomy, and subsequent volume EM, can be performed upon laser carving in the flat-embedded resin sample (left). Alternatively, near-infrared branding (NIRB)-guided marks can be physically drawn on vibratome sections of the mouse brain for guiding ultramicrotomy and/or volume EM (middle). NIRB can also be used for whole-organ ‘tattooing’ (e.g. ear, brain) and thereby guide the biopsy of the region of interest (ROI) in voluminous samples, such as the mouse brain. Resin-embedded ROIs are then scanned by using mCT, the volumes are then registered and the position of the ROIs retrieved; this allows 3DEM by using FIB-SEM (right).

allowed them time-lapse recordings of endocytosis gaining ultrastructural information from resin sections imaged by applying electron tomography (Kukulski et al., 2011, 2012). These elegant studies elucidated how proteins that control membrane budding, such as clathrin, actin and amphiphysin, drive invagination, elongation and fission of endocytic vesicles. Further work using CLEM showed that vesicle budding appears to involve the assembly of clathrin adaptors (Skruzny et al., 2015) and the bending of a dynamic preassembled clathrin coat (Avinoam et al., 2015). Similar approaches of preserving the fluorescence signal have been used in CLEM of zebrafish embryos (Nixon et al., 2009), *C. elegans* (Watanabe et al., 2011) and mammalian cells (Paez-Segala et al., 2015; Peddie et al., 2014). CLEM can also be performed thanks to the development of bimodal probes, such as the mini singlet oxygen generator (miniSOG) (Shu et al., 2011) and proteins of the ascorbate peroxidase (APX) family, in particular APEX2 (Lam et al., 2015). MiniSOG is a fluorescent flavoprotein that, when genetically encoded, is used as a versatile tag that emits fluorescence and, in response to illumination, generates singlet oxygen that transforms diaminobenzidine into electron-dense precipitates that can be imaged by using EM. The engineered peroxidase APEX, by contrast, can be used for EM and proximity labeling upon its fusion to a protein of interest, (Mick et al., 2015). Alternatively, events or regions of interest can be tracked over the two imaging modalities, with recording of coordinates imprinted on the culture dish, by using either commercialized (Al Jord et al., 2014) or laser-micropatterned culture substrates (Spiegelhalter et al., 2010). This method allows the fast freezing (e.g. high-pressure freezing) of dynamic events within seconds for their ultrastructural characterization. A similar approach has recently been used to characterize centriole duplication in multi-ciliated ependymal cells, which grow multiple motile cilia that efficiently propel the cerebrospinal fluid in brain ventricles. By combining live super-resolution imaging of ependymal progenitors by using EM, Al Jord and colleagues could show that multiple centrioles derive from the pre-existing progenitor cell centrosome following multiple rounds of procentriole seeding, thereby unraveling an unexpected centriolar asymmetry that differs from the archetypal duplication program found in other ciliated cells (Al Jord et al., 2014). Similarly, *in vitro* CLEM has been combined with the 3D electron microscopy (3DEM) technique focused ion beam scanning electron microscopy (FIB-SEM) to show that invadopodia of cancer cells potentially mature in response to a mechanical interplay with the nucleus (Revach et al., 2015). Their EM data revealed that invadopodia are composed of actin bundles that interact with and indent the nucleus at the apical side. Finally, many of the issues that are encountered when retrieving the ROI in EM after light microscopy and sample transfer can be avoided by using integrated microscopes that are specially designed for CLEM studies; the latter also allow the combination of atomic force microscopy and EM (for a review see de Boer et al., 2015).

#### CLEM of multicellular and 3D samples – probing biomechanics at high resolution

A major gap in cell biology is to understand cell biological events in a realistic pathophysiological context. This can only be approached by using light microscopy in living animals, i.e. intravital imaging. Although single-photon and light-sheet imaging allow to image small organisms, such as *Drosophila*, *C. elegans* and zebrafish embryos at any depth, the event of interest might be beyond the imaging depth of the fluorescence microscope in higher organisms, such as mice. As discussed above, this can be easily overcome by

surgical implantation of imaging windows and the use of multiphoton microscopy (Helmchen and Denk, 2005), which permits to acquire high-quality fluorescent images deep inside animals (see above).

However, most organs are not directly optically accessible and require surgical procedures to expose the tissue of interest, as is employed in neuroscience (Dombeck et al., 2007) and cancer research (Ellenbroek and van Rheenen, 2014). The second, and biggest, challenge resides in the difficulty to retrieve the ROI in voluminous resin-embedded 3D samples (up to a few mm<sup>3</sup>). In small organisms and embryos, anatomical landmarks, such as fluorescent or visible structures that have been imaged *in vivo* can be utilized to provide key anchor points for pinpointing the event of interest in the resin-embedded tissue (Durdu et al., 2014; Goetz et al., 2014, 2015; Kolotuev et al., 2010, 2013; Müller-Reichert et al., 2007). This has proven to be very useful in zebrafish embryos for correlating the blood flow that is sensed by endothelial cilia to their inner ultrastructure (Fig. 4A,B). In addition to anatomical landmarks, artificial markers can be carved in the resin, which – upon superimposition with the intravital image – facilitate targeted ultramicrotomy by EM. Of note, laser etching had been originally pioneered on glass coverslips for micropatterning-assisted CLEM of cells (Spiegelhalter et al., 2010). In resin- and flat-embedded small organisms, it facilitates the retrieval of a precise ROI located within the intravital image and, for instance, afforded the characterization of how fibroblast growth factor (FGF) activity controls the frequency at which rosette-like mechanosensory organs, e.g. the zebrafish lateral line primordium, are deposited through the assembly of microluminal structures that constrain FGF signaling (Durdu et al., 2014). Studies performed in *C. elegans* provide additional examples of laser-assisted targeted ultramicrotomy; these have helped to further clarify at high resolution the formation of excretory canals, as well as the contribution of exosomes to alae formation (Hyenne et al., 2015) (Fig. 4A). Laser etching can also be used directly on hydrated tissues to precisely locate the ROI. This technology, called near-infrared branding (NIRB) has been developed a few years ago and enables to highlight the position of the ROI, either owing to laser-induced autofluorescence or upon photooxidation of the NIRB mark (Bishop et al., 2011) (Fig. 4B). In that study, by using NIRB on brain vibratome sections, single cortical dendritic spines that had been previously recorded in a living mouse could be dissected at unprecedented resolution (Bishop et al., 2011). Furthermore, NIRB-guided retrieval of the ROI in vibratome sections allows to combine intravital imaging with 3DEM, such as FIB-SEM, which was shown to provide nanoscale isotropic imaging of axons and dendrites (Maco et al., 2013). Combined with state-of-the-art optogenetic tools, intravital CLEM holds great promises for resolving long-standing questions in brain connectivity. For instance, NIRB has recently been customized to perform tissue surface ‘tattooing’, which facilitates the retrieval of the ROI before embedding (Karreman et al., 2014) (Fig. 4B). However, although this approach allows to selectively target the ROI-contained volume in *x* and *y* direction, the *z*-position within the block cannot be estimated from it, and serial sectioning throughout the block is required for ROI retrieval. Combined with anatomical landmarks, NIRB-assisted tattooing of the mouse ear skin was used to precisely correlate intravital imaging of subcutaneous tumors with high-resolution electron tomography (Karreman et al., 2014). However, these techniques do not provide the opportunity to predict where the ROI is within the resin-embedded sample; being able to achieve this would greatly increase throughput and facilitate *en block* imaging, which is of utmost importance when working with

high-volume samples. One way to circumvent this issue is to implement a third imaging modality to map the resin-embedded ROI and thereby predict the position of the ROI by cross-correlating the topology of anatomical landmarks. This opportunity is provided by X-ray micro-computed tomography (microCT), which uses the presence of heavy metals, such as osmium – and which are required for EM – to resolve a number of anatomical structures, such as the vasculature, hair follicles and collagen fibers (Karreman et al., 2016). This approach has been used on brain vibratome sections and allowed to locate photo-oxidized neuronal structures (Bushong et al., 2015). Moreover, microCT can be used on voluminous samples, such as brain biopsies, and allows to accurately resolve the brain capillary architecture. We have recently shown that implementing microCT as an intermediate step between intravital imaging of brain metastasis and FIB-SEM allows the high-resolution imaging of single metastatic cells (Karreman et al., 2016). The combination of state-of-the-art light and intravital microscopy techniques together with the growing approaches for 3DEM will provide scientists with an unprecedented toolbox that can help to resolve – *in vivo* and at very high resolution – many of the current questions surrounding cell biology. We believe that intravital CLEM has the potential to provide the link between cell biology and relevant pathophysiological contexts and, undoubtedly, will become the next-generation microscopy for *in vivo* cell biologists (Table 1).

## Conclusions

We have summarized here the imaging approaches that are currently used for studying any cell biological event of interest. Cell biologists are now in the great position to have access to a wide and still-growing palette of fast, non-invasive, high-resolution, label-free technologies that make true ‘*in vivo* cell biology’ a goal that is within reach in the near future. It is of utmost importance to continue to pursue the development of high-resolution and animal-suitable imaging approaches in order to visualize the cell biology of any given disease within an animal model. This giant leap forward will enable us to model, image, quantify and understand the complexity of cell biology within its most relevant contexts, thereby contributing to the wealth of knowledge and to the design of optimal therapeutic strategies to deal with life-threatening pathologies.

## Acknowledgements

The authors thank all the members of the Goetz lab for useful insights and discussions as well as proofreading.

## Competing interests

The authors declare no competing or financial interests.

## Funding

This work has been supported by research grants from the French National Cancer Institute (Institut National Du Cancer, INCa) and the Ligue Contre le Cancer (J.G.G.), the Plan Cancer, by institutional funding from Institut National de la Santé et de la Recherche Médicale (Inserm) and the Université de Strasbourg (IdeX, investissements d’avenir), and by the LABEx NIE (grant number: ANR-11-LABX-0058\_NIE). L.M. is supported by an INSERM/Région Alsace Ph.D fellowship and G. F. is supported by a Ligue contre le Cancer Ph.D fellowship, N.O. is supported by funding from Plan Cancer.

## References

- Ahmed, W. W., Fodor, É. and Betz, T. (2015). Active cell mechanics: measurement and theory. *Biochim. Biophys. Acta Mol. Cell Res.* **1853**, 3083–3094.
- Ahrens, M. B., Orger, M. B., Robson, D. N., Li, J. M. and Keller, P. J. (2013). Whole-brain functional imaging at cellular resolution using light-sheet microscopy. *Nat. Methods* **10**, 413–420.
- Al Jord, A., Lemaître, A.-I., Delgehr, N., Faucourt, M., Spassky, N. and Meunier, A. (2014). Centriole amplification by mother and daughter centrioles differs in multiciliated cells. *Nature* **516**, 104–107.
- Alexander, S., Weigel, B., Winkler, F. and Friedl, P. (2013). Preclinical intravital microscopy of the tumour-stroma interface: invasion, metastasis, and therapy response. *Curr. Opin. Cell Biol.* **25**, 659–671.
- Allegra Mascaró, A. L., Cesare, P., Sacconi, L., Grasselli, G., Mandolesi, G., Maco, B., Knott, G. W., Huang, L., De Paola, V., Strata, P. et al. (2013). *In vivo* single branch axotomy induces GAP-43-dependent sprouting and synaptic remodeling in cerebellar cortex. *Proc. Natl. Acad. Sci. USA* **110**, 10824–10829.
- Anton, H., Harlepp, S., Ramspacher, C., Wu, D., Monduc, F., Bhat, S., Liebling, M., Paoletti, C., Charvin, G., Freund, J. B. et al. (2013). Pulse propagation by a capacitive mechanism drives embryonic blood flow. *Development* **140**, 4426–4434.
- Ashkin, A. (1997). Optical trapping and manipulation of neutral particles using lasers. *Proc. Natl. Acad. Sci. USA* **94**, 4853–4860.
- Ashkin, A. and Dziedzic, J. (1987). Optical trapping and manipulation of viruses and bacteria. *Science* **235**, 1517–1520.
- Ashkin, A., Dziedzic, J. M. and Yamane, T. (1987). Optical trapping and manipulation of single cells using infrared laser beams. *Nature* **330**, 769–771.
- Avinoum, O., Schorb, M., Beese, C. J., Briggs, J. A. G. and Kaksonen, M. (2015). ENDOCYTOSIS. Endocytic sites mature by continuous bending and remodeling of the clathrin coat. *Science* **348**, 1369–1372.
- Balaban, N. Q., Schwarz, U. S., Riveline, D., Goichberg, P., Tzur, G., Sabanay, I., Mahalu, D., Safran, S., Bershadsky, A., Addadi, L. et al. (2001). Force and focal adhesion assembly: a close relationship studied using elastic micropatterned substrates. *Nat. Cell Biol.* **3**, 466–472.
- Bambardekar, K., Clément, R., Blanc, O., Chardès, C. and Lenne, P.-F. (2015). Direct laser manipulation reveals the mechanics of cell contacts *in vivo*. *Proc. Natl. Acad. Sci. USA* **112**, 1416–1421.
- Berning, S., Willig, K. I., Steffens, H., Dibaj, P. and Hell, S. W. (2012). Nanoscopy in a living mouse brain. *Science* **335**, 551–551.
- Betzig, E., Patterson, G. H., Sougrat, R., Lindwasser, O. W., Olenych, S., Bonifacino, J. S., Davidson, M. W., Lippincott-Schwartz, J. and Hess, H. F. (2006). Imaging intracellular fluorescent proteins at nanometer resolution. *Science* **313**, 1642–1645.
- Bishop, D., Nikić, I., Brinkoetter, M., Knecht, S., Potz, S., Kerschensteiner, M. and Misgeld, T. (2011). Near-infrared branding efficiently correlates light and electron microscopy. *Nat. Methods* **8**, 568–570.
- Boulois, J.-L. (1986). Photophysical processes in recent medical laser developments: a review. *Lasers Med. Sci.* **1**, 47–66.
- Brunet, T., Bouclet, A., Ahmadi, P., Mitrossilis, D., Driquez, B., Brunet, A.-C., Henry, L., Serman, F., Béalle, G., Ménager, C. et al. (2013). Evolutionary conservation of early mesoderm specification by mechanotransduction in Bilateria. *Nat. Commun.* **4**, 2821.
- Bushong, E. A., Johnson, D. D., Kim, K.-Y., Terada, M., Hatori, M., Peltier, S. T., Panda, S., Merkle, A. and Ellisman, M. H. (2015). X-ray microscopy as an approach to increasing accuracy and efficiency of serial block-face imaging of correlated light and electron microscopy of biological specimens. *Microsc. Microanal.* **21**, 231–238.
- Chen, B.-C., Legant, W. R., Wang, K., Shao, L., Milkie, D. E., Davidson, M. W., Janetopoulos, C., Wu, X. S., Hammer, J. A., Liu, Z. et al. (2014). Lattice light-sheet microscopy: imaging molecules to embryos at high spatiotemporal resolution. *Science* **346**, 1257998.
- Chhetri, R. K., Amat, F., Wan, Y., Höckendorf, B., Lemon, W. C. and Keller, P. J. (2015). Whole-animal functional and developmental imaging with isotropic spatial resolution. *Nat. Methods* **12**, 1171–1178.
- Chivukula, V. K., Krog, B. L., Nauseef, J. T., Henry, M. D. and Vigmostad, S. C. (2015). Alterations in cancer cell mechanical properties after fluid shear stress exposure: a micropipette aspiration study. *Cell Health Cytoskeleton* **7**, 25–35.
- Collins, C., Osborne, L. D., Guilluy, C., Chen, Z., O’Brien, E. T., III, Reader, J. S., Burrige, K., Superfine, R. and Tzima, E. (2014). Haemodynamic and extracellular matrix cues regulate the mechanical phenotype and stiffness of aortic endothelial cells. *Nat. Commun.* **5**, 3984.
- Coto Hernández, I., Castello, M., Lanzañò, L., d’Amora, M., Bianchini, P., Diaspro, A. and Vicidomini, G. (2016). Two-photon excitation STED microscopy with time-gated detection. *Sci. Rep.* **6**, 19419.
- Dao, M., Lim, C. T. and Suresh, S. (2003). Mechanics of the human red blood cell deformed by optical tweezers. *J. Mech. Phys. Solids* **51**, 2259–2280.
- de Boer, P., Hoogenboom, J. P. and Giepmans, B. N. G. (2015). Correlated light and electron microscopy: ultrastructure lights up! *Nat. Methods* **12**, 503–513.
- Débarre, D., Supatto, W., Pena, A.-M. M., Fabre, A., Tordjmann, T., Combettes, L., Schanne-Klein, M.-C. and Beaufort, E. (2006). Imaging lipid bodies in cells and tissues using third-harmonic generation microscopy. *Nat. Methods* **3**, 47–53.
- Denk, W., Strickler, J. H. and Webb, W. W. (1990). Two-photon laser scanning fluorescence microscopy. *Science* **248**, 73–76.
- Desprat, N., Supatto, W., Pouille, P.-A., Beaufort, E. and Farge, E. (2008). Tissue deformation modulates twist expression to determine anterior midgut differentiation in *Drosophila* embryos. *Dev. Cell* **15**, 470–477.
- Dombeck, D. A., Khabbaz, A. N., Collman, F., Adelman, T. L. and Tank, D. W. (2007). Imaging large-scale neural activity with cellular resolution in awake, mobile mice. *Neuron* **56**, 43–57.

- Durdu, S., Iskar, M., Revenu, C., Schieber, N., Kunze, A., Bork, P., Schwab, Y. and Gilmour, D. (2014). Luminal signalling links cell communication to tissue architecture during organogenesis. *Nature* **515**, 120-124.
- Ellenbroek, S. I. J. and van Rheenen, J. (2014). Imaging hallmarks of cancer in living mice. *Nat. Rev. Cancer* **14**, 406-418.
- Eyckmans, J., Boudou, T., Yu, X. and Chen, C. S. (2011). A Hitchhiker's guide to mechanobiology. *Dev. Cell* **21**, 35-47.
- Fiolka, R., Shao, L., Rego, E. H., Davidson, M. W. and Gustafsson, M. G. L. (2012). Time-lapse two-color 3D imaging of live cells with doubled resolution using structured illumination. *Proc. Natl. Acad. Sci. USA* **109**, 5311-5315.
- Franken, P. A., Hill, A. E., Peters, C. W. and Weinreich, G. (1963). Generation of optical harmonics. *Phys. Rev. Lett.* **118**.
- Friedrich, M. and Harms, G. S. (2015). Axial resolution beyond the diffraction limit of a sheet illumination microscope with stimulated emission depletion. *J. Biomed. Opt.* **20**, 106006-106006.
- Friedrich, M., Gan, Q., Ermolayev, V. and Harms, G. S. (2011). STED-SPIM: stimulated emission depletion improves sheet illumination microscopy resolution. *Biophys. J.* **100**, L43-L45.
- Gao, L., Shao, L., Higgins, C. D., Poulton, J. S., Peifer, M., Davidson, M. W., Wu, X., Goldstein, B. and Betzig, E. (2012). Noninvasive imaging beyond the diffraction limit of 3D dynamics in thickly fluorescent specimens. *Cell* **151**, 1370-1385.
- Goetz, J. G., Steed, E., Ferreira, R. R., Roth, S., Ramsbacher, C., Boselli, F., Charvin, G., Liebling, M., Wyart, C., Schwab, Y. et al. (2014). Endothelial cilia mediate low flow sensing during zebrafish vascular development. *Cell Rep.* **6**, 799-808.
- Goetz, J. G., Monduc, F., Schwab, Y. and Vermot, J. (2015). Using correlative light and electron microscopy to study zebrafish vascular morphogenesis. *Methods Mol. Biol.* **1189**, 31-46.
- Göppert-Mayer, M. (1931). Über Elementarakt mit zwei Quantensprüngen. *Ann. Phys.* **401**, 273-294.
- Grange, R., Lanvin, T., Hsieh, C.-L., Pu, Y. and Psaltis, D. (2011). Imaging with second-harmonic radiation probes in living tissue. *Biomed. Opt. Express* **2**, 2532-2539.
- Graves, E. T., Duboc, C., Fan, J., Stransky, F., Leroux-Coyau, M. and Strick, T. R. (2015). A dynamic DNA-repair complex observed by correlative single-molecule nanomanipulation and fluorescence. *Nat. Struct. Mol. Biol.* **22**, 452-457.
- Guevorkian, K., Colbert, M.-J., Durth, M., Dufour, S. and Brochard-Wyart, F. (2010). Aspiration of biological viscoelastic drops. *Phys. Rev. Lett.* **104**, 218101.
- Guevorkian, K., Gonzalez-Rodriguez, D., Carlier, C., Dufour, S. and Brochard-Wyart, F. (2011). Mechanosensitive shivering of model tissues under controlled aspiration. *Proc. Natl. Acad. Sci. USA* **108**, 13387-13392.
- Guiliak, F., Tedrow, J. R. and Burgkart, R. (2000). Viscoelastic properties of the cell nucleus. *Biochem. Biophys. Res. Commun.* **269**, 781-786.
- Gupta, M., Kocgozlu, L., Sarangi, B. R., Margadant, F., Ashraf, M. and Ladoux, B. (2015). Micropillar substrates: a tool for studying cell mechanobiology. *Methods Cell Biol.* **125**, 289-308.
- Gustafsson, M. G. L. (2000). Surpassing the lateral resolution limit by a factor of two using structured illumination microscopy. *J. Microsc.* **198**, 82-87.
- Gustafsson, M. G. L., Shao, L., Carlton, P. M., Wang, C. J. R., Golubovskaya, I. N., Cande, W. Z., Agard, D. A. and Sedat, J. W. (2008). Three-dimensional resolution doubling in wide-field fluorescence microscopy by structured illumination. *Biophys. J.* **94**, 4957-4970.
- Hajji, B., Wisniewski, J., El Beheiry, M., Chen, J., Revyakin, A., Wu, C. and Dahan, M. (2014). Whole-cell, multicolor superresolution imaging using volumetric multifocus microscopy. *Proc. Natl. Acad. Sci. USA* **111**, 17480-17485.
- Headley, M. B., Bins, A., Nip, A., Roberts, E. W., Looney, M. R., Gerard, A. and Krummel, M. F. (2016). Visualization of immediate immune responses to pioneer metastatic cells in the lung. *Nature* **531**, 513-517.
- Heilemann, M., Margeat, E., Kasper, R., Sauer, M. and Tinnefeld, P. (2005). Carbocyanine dyes as efficient reversible single-molecule optical switch. *J. Am. Chem. Soc.* **127**, 3801-3806.
- Heilemann, M., van de Linde, S., Schüttelpelz, M., Kasper, R., Seefeldt, B., Mukherjee, A., Tinnefeld, P. and Sauer, M. (2008). Subdiffraction-resolution fluorescence imaging with conventional fluorescent probes. *Angew. Chem. Int. Ed.* **47**, 6172-6176.
- Heinlein, T., Biebricher, A., Schlüter, P., Roth, C. M., Herten, D.-P., Wolfrum, J., Heilemann, M., Müller, C., Tinnefeld, P. and Sauer, M. (2005). High-resolution colocalization of single molecules within the resolution gap of far-field microscopy. *ChemPhysChem* **6**, 949-955.
- Hellerer, T., Axäng, C., Brackmann, C., Hillertz, P., Pilon, M. and Enejder, A. (2007). Monitoring of lipid storage in *Caenorhabditis elegans* using coherent anti-Stokes Raman scattering (CARS) microscopy. *Proc. Natl. Acad. Sci. USA* **104**, 14658-14663.
- Hellström, K., Vihinen, H., Kallio, K., Jokitalo, E. and Ahola, T. (2015). Correlative light and electron microscopy enables viral replication studies at the ultrastructural level. *Methods* **90**, 49-56.
- Helmchen, F. and Denk, W. (2005). Deep tissue two-photon microscopy. *Nat. Methods* **2**, 932-940.
- Hess, S. T., Girirajan, T. P. K. and Mason, M. D. (2006). Ultra-high resolution imaging by fluorescence photoactivation localization microscopy. *Biophys. J.* **91**, 4258-4272.
- Hochmuth, R. M. (2000). Micropipette aspiration of living cells. *J. Biomech.* **33**, 15-22.
- Hoffman, B. D., Grashoff, C. and Schwartz, M. A. (2011). Dynamic molecular processes mediate cellular mechanotransduction. *Nature* **475**, 316-323.
- Hoyer, P., de Medeiros, G., Balázs, B., Norlin, N., Besir, C., Hanne, J., Kräusslich, H.-G., Engelhardt, J., Sahl, S. J., Hell, S. W. et al. (2016). Breaking the diffraction limit of light-sheet fluorescence microscopy by RESOLFT. *Proc. Natl. Acad. Sci. USA* **113**, 3442-3446.
- Huang, F., Hartwich, T. M. P., Rivera-Molina, F. E., Lin, Y., Duim, W. C., Long, J. J., Uchil, P. D., Myers, J. R., Baird, M. A., Mothes, W. et al. (2013). Video-rate nanoscopy using sCMOS camera-specific single-molecule localization algorithms. *Nat. Methods* **10**, 653-658.
- Huisken, J., Swoger, J., Bene, F. D., Wittbrodt, J. and Stelzer, E. H. K. (2004). Optical sectioning deep inside live embryos by selective plane illumination microscopy. *Science* **305**, 1007-1009.
- Hyenne, V., Apaydin, A., Rodriguez, D., Spiegelhalter, C., Hoff-Yoessle, S., Diem, M., Tak, S., Lefebvre, O., Schwab, Y., Goetz, J. G. et al. (2015). RAL-1 controls multivesicular body biogenesis and exosome secretion. *J. Cell Biol.* **211**, 27-37.
- Jakob, P. H., Kehrler, J., Flood, P., Wiegel, C., Haselmann, U., Meissner, M., Stelzer, E. H. K. and Reynaud, E. G. (2016). A 3-D cell culture system to study epithelia functions using microcarriers. *Cytotechnology*. [Epub ahead of print] doi:10.1007/s10616-015-9935-0
- Janmey, P. A. and Miller, R. T. (2011). Mechanisms of mechanical signaling in development and disease. *J. Cell Sci.* **124**, 9-18.
- Jenne, C. N., Wong, C. H. Y., Petri, B. and Kubes, P. (2011). The use of spinning-disk confocal microscopy for the intravital analysis of platelet dynamics in response to systemic and local inflammation. *6*, e25109.
- Juette, M. F., Gould, T. J., Lessard, M. D., Mlodzionoski, M. J., Nagpure, B. S., Bennett, B. T., Hess, S. T. and Bewersdorff, J. (2008). Three-dimensional sub-100 nm resolution fluorescence microscopy of thick samples. *Nat. Methods* **5**, 527-529.
- Karreman, M. A., Mercier, L., Schieber, N. L., Shibue, T., Schwab, Y. and Goetz, J. G. (2014). Correlating intravital multi-photon microscopy to 3D electron microscopy of invading tumor cells using anatomical reference points. *PLoS ONE* **9**, e114448.
- Karreman, M. A., Mercier, L., Schieber, N. L., Solecki, G., Allio, G., Winkler, F., Ruthensteiner, B., Goetz, J. G. and Schwab, Y. (2016). Fast and precise targeting of single tumor cells in vivo by multimodal correlative microscopy. *J. Cell Sci.* **129**, 444-456.
- Keller, P. J. and Ahrens, M. B. (2015). Visualizing whole-brain activity and development at the single-cell level using light-sheet microscopy. *Neuron* **85**, 462-483.
- Keller, P. J., Schmidt, A. D., Wittbrodt, J. and Stelzer, E. H. K. (2008). Reconstruction of Zebrafish early embryonic development by scanned light sheet microscopy. *Science* **322**, 1065-1069.
- Khare, S. M., Awasthi, A., Venkataraman, V. and Koushika, S. P. (2015). Colored polydimethylsiloxane micropillar arrays for high throughput measurements of forces applied by genetic model organisms. *Biomicrofluidics* **9**, 014111.
- Kienast, Y., von Baumgarten, L., Fuhrmann, M., Klinkert, W. E. F., Goldbrunner, R., Herms, J. and Winkler, F. (2010). Real-time imaging reveals the single steps of brain metastasis formation. *Nat. Med.* **16**, 116-122.
- Kim, D.-H., Wong, P. K., Park, J., Levchenko, A. and Sun, Y. (2009). Microengineered Platforms for Cell Mechanobiology. *Annu. Rev. Biomed. Eng.* **11**, 203-233.
- Kissa, K. and Herbomel, P. (2010). Blood stem cells emerge from aortic endothelium by a novel type of cell transition. *Nature* **464**, 112-115.
- Klajnner, M., Hebraud, P., Sirlin, C., Gaiddon, C. and Harlepp, S. (2010). DNA binding to an anticancer Organo-Ruthenium complex. *J. Phys. Chem. B* **114**, 14041-14047.
- Klar, T. A., Jakobs, S., Dyba, M., Egner, A. and Hell, S. W. (2000). Fluorescence microscopy with diffraction resolution barrier broken by stimulated emission. *Proc. Natl. Acad. Sci. USA* **97**, 8206-8210.
- Kner, P., Chhun, B. B., Griffis, E. R., Winoto, L. and Gustafsson, M. G. L. (2009). Super-resolution video microscopy of live cells by structured illumination. *Nat. Methods* **6**, 339-342.
- Kobat, D., Horton, N. G. and Xu, C. (2011). In vivo two-photon microscopy to 1.6-mm depth in mouse cortex. *J. Biomed. Opt.* **16**, 106014.
- Kolotuev, I., Schwab, Y. and Labouesse, M. (2010). A precise and rapid mapping protocol for correlative light and electron microscopy of small invertebrate organisms. *Biol. Cell* **102**, 121-132.
- Kolotuev, I., Hyenne, V., Schwab, Y., Rodriguez, D. and Labouesse, M. (2013). A pathway for unicellular tube extension depending on the lymphatic vessel determinant Prox1 and on osmoregulation. *Nat. Cell Biol.* **15**, 157-168.
- Krzic, U., Gunther, S., Saunders, T. E., Streichan, S. J. and Hufnagel, L. (2012). Multiview light-sheet microscope for rapid in toto imaging. *Nat. Methods* **9**, 730-733.

- Kukulski, W., Schorb, M., Welsch, S., Picco, A., Kaksonen, M. and Briggs, J. A. G. (2011). Correlated fluorescence and 3D electron microscopy with high sensitivity and spatial precision. *J. Cell Biol.* **192**, 111–119.
- Kukulski, W., Schorb, M., Kaksonen, M. and Briggs, J. A. G. (2012). Plasma membrane reshaping during endocytosis is revealed by time-resolved electron tomography. *Cell* **150**, 508–520.
- Kuznetsova, T. G., Starodubtseva, M. N., Yegorenkov, N. I., Chizhik, S. A. and Zhdanov, R. I. (2007). Atomic force microscopy probing of cell elasticity. *Micron* **38**, 824–833.
- Lam, S. S., Martell, J. D., Kamer, K. J., Deerinck, T. J., Ellisman, M. H., Mootha, V. K. and Ting, A. Y. (2015). Directed evolution of APEX2 for electron microscopy and proximity labeling. *Nat. Methods* **12**, 51–54.
- Lanzicher, T., Martinelli, V., Puzzi, L., Del Favero, G., Codan, B., Long, C. S., Mestroni, L., Taylor, M. R. G. and Sbaizero, O. (2015). The cardiomyopathy lamin A/C D192G mutation disrupts whole-cell biomechanics in cardiomyocytes as measured by atomic force microscopy loading-unloading curve analysis. *Sci. Rep.* **5**, 13388.
- Lee, M., Downes, A., Chau, Y.-Y., Serrels, B., Hastie, N., Elfick, A., Brunton, V., Frame, M. and Serrels, A. (2015). In vivo imaging of the tumor and its associated microenvironment using combined CARS/2-photon microscopy. *IntraVital* **4**, e1055430.
- Legant, W. R., Shao, L., Grimm, J. B., Brown, T. A., Milkie, D. E., Avants, B. B., Lavis, L. D. and Betzig, E. (2016). High-density three-dimensional localization microscopy across large volumes. *Nat. Methods* **13**, 359–365.
- Li, J. L., Goh, C. C., Keeble, J. L., Qin, J. S., Roediger, B., Jain, R., Wang, Y., Chew, W. K., Weninger, W. and Ng, L. G. (2012). Intravital multiphoton imaging of immune responses in the mouse ear skin. *Nat. Protoc.* **7**, 221–234.
- Li, D., Shao, L., Chen, B.-C., Zhang, X., Zhang, M., Moses, B., Milkie, D. E., Beach, J. R., Hammer, J. A., Pasham, M. et al. (2015). Extended-resolution structured illumination imaging of endocytic and cytoskeletal dynamics. *Science* **349**, aab3500.
- Lim, J., Lee, H. K., Yu, W. and Ahmed, S. (2014). Light sheet fluorescence microscopy (LSFM): past, present and future. *Analyst* **139**, 4758–4768.
- Liu, Y.-J., Le Berre, M., Lautenschlaeger, F., Maiuri, P., Callan-Jones, A., Heuzé, M., Takaki, T., Voituriez, R. and Piel, M. (2015). Confinement and low adhesion induce fast amoeboid migration of slow mesenchymal cells. *Cell* **160**, 659–672.
- Lye, C. M., Blanchard, G. B., Naylor, H. W., Muresan, L., Huisken, J., Adams, R. J. and Sanson, B. (2015). Mechanical coupling between endoderm invagination and axis extension in *Drosophila*. *PLoS Biol.* **13**, e1002292.
- Maco, B., Holtmaat, A., Cantoni, M., Kreshuk, A., Straehle, C. N., Hamprecht, F. A. and Knott, G. W. (2013). Correlative in vivo 2 photon and focused ion beam scanning electron microscopy of cortical neurons. *PLoS ONE* **8**, e57405.
- Maker, P. D. and Terhune, R. W. (1965). Study of optical effects due to an induced polarization third order in the electric field strength. *Phys. Rev.* **137**, 801–818.
- Manley, S., Gillette, J. M., Patterson, G. H., Shroff, H., Hess, H. F., Betzig, E. and Lippincott-Schwartz, J. (2008). High-density mapping of single-molecule trajectories with photoactivated localization microscopy. *Nat. Methods* **5**, 155–157.
- Mao, Y., Sun, Q., Wang, X., Ouyang, Q., Han, L., Jiang, L. and Han, D. (2009). In vivo nanomechanical imaging of blood-vessel tissues directly in living mammals using atomic force microscopy. *Appl. Phys. Lett.* **95**, 013704.
- Marjoram, R. J., Guilly, C. and Burridge, K. (2016). Using magnets and magnetic beads to dissect signaling pathways activated by mechanical tension applied to cells. *Methods* **94**, 19–26.
- Masedunskas, A., Milberg, O., Porat-Shliom, N., Sramkova, M., Wigand, T., Amornphimoltham, P. and Weigert, R. (2012). Intravital microscopy: a practical guide on imaging intracellular structures in live animals. *BioArchitecture* **2**, 143–157.
- Mercier, L., Böhm, J., Fekonja, N., Allio, G., Lutz, Y., Koch, M., Goetz, J. G. and Laporte, J. (2016). In vivo imaging of skeletal muscle in mice highlights muscle defects in a mouse model of myotubular myopathy. *IntraVital* **5**, e1168553.
- Mick, D. U., Rodrigues, R. B., Leib, R. D., Adams, C. M., Chien, A. S., Gygi, S. P. and Nachury, M. V. (2015). Proteomics of primary cilia by proximity labeling. *Dev. Cell* **35**, 497–512.
- Mickoleit, M., Schmid, B., Weber, M., Fahrback, F. O., Hombach, S., Reischauer, S. and Huisken, J. (2014). High-resolution reconstruction of the beating zebrafish heart. *Nat. Methods* **11**, 919–922.
- Minsky, M. (1961). Microscopy apparatus. U.S. Patent 3,013,467.
- Müller-Reichert, T., Srayko, M., Hyman, A., O'Toole, E. T. and McDonald, K. (2007). Correlative light and electron microscopy of early *Caenorhabditis elegans* embryos in mitosis. *Methods Cell Biol.* **79**, 101–119.
- Neuman, K. C. and Nagy, A. (2008). Single-molecule force spectroscopy: optical tweezers, magnetic tweezers and atomic force microscopy. *Nat. Methods* **5**, 491–505.
- Nguyen, J. P., Shipley, F. B., Linder, A. N., Plummer, G. S., Liu, M., Setru, S. U., Shaevitz, J. W. and Leifer, A. M. (2016). Whole-brain calcium imaging with cellular resolution in freely behaving *Caenorhabditis elegans*. *Proc. Natl. Acad. Sci. USA* **113**, E1074–E1081.
- Nixon, S. J., Webb, R. I., Floetenmeyer, M., Schieber, N., Lo, H. P. and Parton, R. G. (2009). A single method for cryofixation and correlative light, electron microscopy and tomography of zebrafish embryos. *Traffic* **10**, 131–136.
- Ossola, D., Amarouch, M.-Y., Behr, P., Vörös, J., Abriel, H. and Zambelli, T. (2015). Force-controlled patch clamp of beating cardiac cells. *Nano Lett.* **15**, 1743–1750.
- Paez-Segala, M. G., Sun, M. G., Shtengel, G., Viswanathan, S., Baird, M. A., Macklin, J. J., Patel, R., Allen, J. R., Howe, E. S., Piszczek, G. et al. (2015). Fixation-resistant photoactivatable fluorescent proteins for CLEM. *Nat. Methods* **12**, 215–218, 4 p following 218.
- Pampaloni, F., Chang, B.-J. and Stelzer, E. H. K. (2015). Light sheet-based fluorescence microscopy (LSFM) for the quantitative imaging of cells and tissues. *Cell Tissue Res.* **360**, 129–141.
- Pantazis, P., Maloney, J., Wu, D. and Fraser, S. E. (2010). Second harmonic generating (SHG) nanoprobe for in vivo imaging. *Proc. Natl. Acad. Sci. USA* **107**, 14535–14540.
- Paszek, M. J., DuFort, C. C., Rossier, O., Bainer, R., Mouw, J. K., Godula, K., Hudak, J. E., Lakins, J. N., Wijekoon, A. C., Cassereau, L. et al. (2014). The cancer glycocalyx mechanically primes integrin-mediated growth and survival. *Nature* **511**, 319–325.
- Peddie, C. J., Liv, N., Hoogenboom, J. P. and Collinson, L. M. (2014). Integrated light and scanning electron microscopy of GFP-expressing cells. *Methods Cell Biol.* **124**, 363–389.
- Peralta, M., Steed, E., Harlepp, S., González-Rosa, J. M., Monduc, F., Ariza-Cosano, A., Cortés, A., Rayón, T., Gómez-Skarmeta, J.-L., Zapata, A. et al. (2013). Heartbeat-driven pericardial fluid forces contribute to epicardium morphogenesis. *Curr. Biol.* **23**, 1726–1735.
- Pérez-Alvarez, A., Araque, A. and Martín, E. D. (2013). Confocal microscopy for astrocyte in vivo imaging: recycle and reuse in microscopy. *Front. Cell Neurosci.* **7**, 51.
- Perrault, C. M., Brugués, A., Bazellieres, E., Ricco, P., Lacroix, D. and Trepast, X. (2015). Traction forces of endothelial cells under slow shear flow. *Biophys. J.* **109**, 1533–1536.
- Peticolas, W. L., Goldsborough, J. P. and Rieckhoff, K. E. (1963). Double photon excitation in organic crystals. *Phys. Rev. Lett.* **10**, 43–45.
- Planchon, T. A., Gao, L., Milkie, D. E., Davidson, M. W., Galbraith, J. A., Galbraith, C. G. and Betzig, E. (2011). Rapid three-dimensional isotropic imaging of living cells using Bessel beam plane illumination. *Nat. Methods* **8**, 417–423.
- Plodinec, M., Loparic, M., Monnier, C. A., Obermann, E. C., Zanetti-Dallenbach, R., Oertle, P., Hyotyla, J. T., Aebi, U., Bentires-Alj, M., Lim, R. Y. and Schoenenberger, C. A. (2012). *Nat. Nanotechnol.* **11**, 57–65.
- Raab, M., Gentili, M., de Belly, H., Thiam, H. R., Vargas, P., Jimenez, A. J., Lautenschlaeger, F., Voituriez, R., Lennon-Duménil, A. M., Manel, N. et al. (2016). ESCRT III repairs nuclear envelope ruptures during cell migration to limit DNA damage and cell death. *Science* **352**, 359–362.
- Raman, C. V. and Krishnan, K. S. (1928). A new type of secondary radiation. *Nature* **121**, 501–502.
- Ramspacher, C., Steed, E., Boselli, F., Ferreira, R., Faggianelli, N., Roth, S., Spiegelhalter, C., Messaddeq, N., Trinh, L., Liebling, M. et al. (2015). Developmental alterations in heart biomechanics and skeletal muscle function in desmin mutants suggest an early pathological root for desminopathies. *Cell Rep.* **11**, 1564–1576.
- Rankin, B. R., Moneron, G., Wurm, C. A., Nelson, J. C., Walter, A., Schwarzer, D., Schroeder, J., Colón-Ramos, D. A. and Hell, S. W. (2011). Nanoscopy in a living multicellular organism expressing GFP. *Biophys. J.* **100**, L63–L65.
- Rego, E. H., Shao, L., Macklin, J. J., Winoto, L., Johansson, G. A., Kamps-Hughes, N., Davidson, M. W. and Gustafsson, M. G. L. (2012). Nonlinear structured-illumination microscopy with a photoswitchable protein reveals cellular structures at 50-nm resolution. *Proc. Natl. Acad. Sci. USA* **109**, E135–E143.
- Revach, O.-Y., Weiner, A., Rechav, K., Sabanay, I., Livne, A. and Geiger, B. (2015). Mechanical interplay between invadopodia and the nucleus in cultured cancer cells. *Sci. Rep.* **5**, 9466.
- Reynaud, E. G., Kržič, U., Greger, K. and Stelzer, E. H. K. (2008). Light sheet-based fluorescence microscopy: more dimensions, more photons, and less photodamage. *HFSP J.* **2**, 266–275.
- Ritsma, L., Steller, E. J. A., Beerling, E., Loomans, C. J. M., Zomer, A., Gerlach, C., Vrisekoop, N., Seinstra, D., van Gorp, L., Schäfer, R. et al. (2012). Intravital microscopy through an abdominal imaging window reveals a pre-metastasis stage during liver metastasis. *Sci. Transl. Med.* **4**, 158ra145.
- Ritsma, L., Ellenbroek, S. I. J., Zomer, A., Snippert, H. J., de Sauvage, F. J., Simons, B. D., Clevers, H. and van Rheenen, J. (2014). Intestinal crypt homeostasis revealed at single-stem-cell level by in vivo live imaging. *Nature* **507**, 362–365.
- Rossier, O., Octeau, V., Sibarita, J.-B., Leduc, C., Tessier, B., Nair, D., Gatterdam, V., Destaing, O., Albignès-Rizo, C., Tampé, R. et al. (2012). Integrins  $\beta 1$  and  $\beta 3$  exhibit distinct dynamic nanoscale organizations inside focal adhesions. *Nat. Cell Biol.* **14**, 1057–1067.

- Rust, M. J., Bates, M. and Zhuang, X. (2006). Sub-diffraction-limit imaging by stochastic optical reconstruction microscopy (STORM). *Nat. Methods* **3**, 793–796.
- Salerno, D., Brogioli, D., Cassina, V., Turchi, D., Beretta, G. L., Seruggia, D., Ziano, R., Zunino, F. and Mantegazza, F. (2010). Magnetic tweezers measurements of the nanomechanical properties of DNA in the presence of drugs. *Nucleic Acids Res.* **38**, 7089–7099.
- Scheul, T., Wang, I. and Vial, J.-C. (2014). STED-SPIM made simple. *Opt. Express* **22**, 30852.
- Schneider, J., Zahn, J., Maglione, M., Sigrist, S. J., Marquard, J., Chojnacki, J., Krüsslich, H.-G., Sahl, S. J., Engelhardt, J. and Hell, S. W. (2015). Ultrafast, temporally stochastic STED nanoscopy of millisecond dynamics. *Nat. Methods* **12**, 827–830.
- Schwarz, U. S. and Soiné, J. R. D. (2015). Traction force microscopy on soft elastic substrates: a guide to recent computational advances. *Biochim. Biophys. Acta Mol. Cell Res.* **1853**, 3095–3104.
- Shao, L., Kner, P., Rego, E. H. and Gustafsson, M. G. L. (2011). Super-resolution 3D microscopy of live whole cells using structured illumination. *Nat. Methods* **8**, 1044–1046.
- Shimozawa, T., Yamagata, K., Kondo, T., Hayashi, S., Shitamukai, A., Konno, D., Matsuzaki, F., Takayama, J., Onami, S., Nakayama, H. et al. (2013). Improving spinning disk confocal microscopy by preventing pinhole cross-talk for intravital imaging. *Proc. Natl. Acad. Sci. USA* **110**, 3399–3404.
- Shu, X., Lev-Ram, V., Deerinck, T. J., Qi, Y., Ramko, E. B., Davidson, M. W., Jin, Y., Ellisman, M. H. and Tsien, R. Y. (2011). A genetically encoded tag for correlated light and electron microscopy of intact cells, tissues, and organisms. *PLoS Biol.* **9**, e1001041.
- Skruzny, M., Desfosses, A., Prinz, S., Dodonova, S. O., Gieras, A., Uetrecht, C., Jakobi, A. J., Abella, M., Hagen, W. J. H., Schulz, J. et al. (2015). An organized co-assembly of clathrin adaptors is essential for endocytosis. *Dev. Cell* **33**, 150–162.
- Smith, S. B., Cui, Y. and Bustamante, C. (1996). Overstretching B-DNA: the elastic response of individual double-stranded and single-stranded DNA molecules. *Science* **271**, 795–799.
- Spiegelhalter, C., Tosch, V., Hentsch, D., Koch, M., Kessler, P., Schwab, Y. and Laporte, J. (2010). From dynamic live cell imaging to 3D ultrastructure: novel integrated methods for high pressure freezing and correlative light-electron microscopy. *PLoS ONE* **5**, e9014.
- Stegmaier, J., Amat, F., Lemon, W. C., McDole, K., Wan, Y., Teodoro, G., Mikut, R. and Keller, P. J. (2016). Real-time three-dimensional cell segmentation in large-scale microscopy data of developing embryos. *Dev. Cell* **36**, 225–240.
- Strick, T. R., Allemand, J.-F., Bensimon, D., Bensimon, A. and Croquette, V. (1996). The elasticity of a single supercoiled DNA molecule. *Science* **271**, 1835–1837.
- Sugimura, K., Lenne, P.-F. and Graner, F. (2016). Measuring forces and stresses in situ in living tissues. *Development* **143**, 186–196.
- Takasaki, K. T., Ding, J. B. and Sabatini, B. L. (2013). Live-cell superresolution imaging by pulsed STED two-photon excitation microscopy. *Biophys. J.* **104**, 770–777.
- Tanase, M., Biais, N. and Sheetz, M. (2007). Magnetic tweezers in cell biology. *Methods Cell Biol.* **83**, 473–493.
- Tartibi, M., Liu, Y. X., Liu, G.-Y. and Komvopoulos, K. (2015). Single-cell mechanics – An experimental–computational method for quantifying the membrane–cytoskeleton elasticity of cells. *Acta Biomater.* **27**, 224–235.
- Tello, M., Spenlé, C., Hemmerlé, J., Mercier, L., Fabre, R., Allio, G., Simon-Assmann, P. and Goetz, J. G. (2016). Generating and characterizing the mechanical properties of cell-derived matrices using atomic force microscopy. *Methods* **94**, 85–100.
- Theer, P., Hasan, M. T. and Denk, W. (2003). Two-photon imaging to a depth of 1000  $\mu\text{m}$  in living brains by use of a Ti:Al<sub>2</sub>O<sub>3</sub> regenerative amplifier. **28**, 1022–1024.
- Théry, M., Pépin, A., Dresseire, E., Chen, Y. and Bornens, M. (2006). Cell distribution of stress fibres in response to the geometry of the adhesive environment. *Cell Motil. Cytoskeleton* **63**, 341–355.
- Thiam, H.-R., Vargas, P., Carpi, N., Crespo, C. L., Raab, M., Terriac, E., King, M. C., Jacobelli, J., Alberts, A. S., Stradal, T. et al. (2016). Perinuclear Arp2/3-driven actin polymerization enables nuclear deformation to facilitate cell migration through complex environments. *Nat. Commun.* **7**, 10997.
- Tomer, R., Khairy, K., Amat, F. and Keller, P. J. (2012). Quantitative high-speed imaging of entire developing embryos with simultaneous multiview light-sheet microscopy. *Nat. Methods* **9**, 755–763.
- Truong, T. V., Supatto, W., Koos, D. S., Choi, J. M. and Fraser, S. E. (2011). Deep and fast live imaging with two-photon scanned light-sheet microscopy. *Nat. Methods* **8**, 757–760.
- Truong Quang, B.-A., Mani, M., Markova, O., Lecuit, T. and Lenne, P.-F. (2013). Principles of E-cadherin supramolecular organization in vivo. *Curr. Biol.* **23**, 2197–2207.
- Vangindertael, J., Beets, I., Rocha, S., Dedecker, P., Schoofs, L., Vanhoorelbeeke, K., Hofkens, J. and Mizuno, H. (2015). Super-resolution mapping of glutamate receptors in *C. elegans* by confocal correlated PALM. *Sci. Rep.* **5**, 13532.
- Vartanian, K. B., Kirkpatrick, S. J., Hanson, S. R. and Hinds, M. T. (2008). Endothelial cell cytoskeletal alignment independent of fluid shear stress on micropatterned surfaces. *Biochem. Biophys. Commun.* **371**, 787–792.
- Versaevol, M., Grevesse, T. and Gabriele, S. (2012). Spatial coordination between cell and nuclear shape within micropatterned endothelial cells. *Nat. Commun.* **3**, 671.
- Vicidomini, G., Moneron, G., Han, K. Y., Westphal, V., Ta, H., Reuss, M., Engelhardt, J., Eggeling, C. and Hell, S. W. (2011). Sharper low-power STED nanoscopy by time gating. *Nat. Methods* **8**, 571–573.
- Villringer, A., Them, A., Lindauer, U., Einhaupl, K. and Dirnagl, U. (1994). Capillary perfusion of the rat brain cortex. *Circ. Res.* **75**, 55–62.
- Wang, W., Wyckoff, J. B., Frohlich, V. C., Oleynikov, Y., Hüttelmaier, S., Zavadil, J., Cermak, L., Bottinger, E. P., Singer, R. H., White, J. G. et al. (2002). Single cell behavior in metastatic primary mammary tumors correlated with gene expression patterns revealed by molecular profiling. *Cancer Res.* **62**, 6278–6288.
- Watanabe, S., Punge, A., Hollopeter, G., Willig, K. I., Hobson, R. J., Davis, M. W., Hell, S. W. and Jorgensen, E. M. (2011). Protein localization in electron micrographs using fluorescence nanoscopy. *Nat. Methods* **8**, 80–84.
- Weber, M. and Huisken, J. (2011). Light sheet microscopy for real-time developmental biology. *Curr. Opin. Genet. Dev.* **21**, 566–572.
- Weigelin, B., Bakker, G.-J. and Friedl, P. (2016). Third harmonic generation microscopy of cells and tissue organization. *J. Cell Sci.* **129**, 245–255.
- Weishart, K. (2014). The basic principle of airyscanning. *Zeiss*.
- Welf, E. S., Driscoll, M. K., Dean, K. M., Schäfer, C., Chu, J., Davidson, M. W., Lin, M. Z., Danuser, G. and Fiolka, R. (2016). Quantitative multiscale cell imaging in controlled 3D microenvironments. *Dev. Cell* **36**, 462–475.
- Westphal, V., Rizzoli, S. O., Lauterbach, M. A., Kamin, D., Jahn, R. and Hell, S. W. (2008). Video-rate far-field optical nanoscopy dissects synaptic vesicle movement. *Science* **320**, 246–249.
- Willig, K. I., Harke, B., Medda, R. and Hell, S. W. (2007). STED microscopy with continuous wave beams. *Nat. Methods* **4**, 915–918.
- Willig, K. I., Steffens, H., Gregor, C., Herholt, A., Rossner, M. J. and Hell, S. W. (2014). Nanoscopy of filamentous actin in cortical dendrites of a living mouse. *Biophys. J.* **106**, L01–L03.
- Wolf, S., Supatto, W., Debrégeas, G., Mahou, P., Kruglik, S. G., Sintes, J.-M., Beaurepaire, E. and Candelier, R. (2015). Whole-brain functional imaging with two-photon light-sheet microscopy. *Nat. Methods* **12**, 379–380.
- Xiao, Y., Faucherre, A., Pola-Morell, L., Heddleston, J. M., Liu, T.-L., Chew, T.-L., Sato, F., Sehara-Fujisawa, A., Kawakami, K. and López-Schier, H. (2015). High-resolution live imaging reveals axon-glia interactions during peripheral nerve injury and repair in zebrafish. *Dis. Model. Mech.* **8**, 553–564.
- Yamashita, N., Morita, M., Legant, W. R., Chen, B.-C., Betzig, E., Yokota, H. and Mimori-Kiyosue, Y. (2015). Three-dimensional tracking of plus-tips by lattice light-sheet microscopy permits the quantification of microtubule growth trajectories within the mitotic apparatus. *J. Biomed. Opt.* **20**, 101206–101206.
- York, A. G., Parekh, S. H., Nogare, D. D., Fischer, R. S., Temprine, K., Mione, M., Chitnis, A. B., Combs, C. A. and Shroff, H. (2012). Resolution doubling in live, multicellular organisms via multifocal structured illumination microscopy. *Nat. Methods* **9**, 749–754.
- York, A. G., Chandris, P., Nogare, D. D., Head, J., Wawrzusin, P., Fischer, R. S., Chitnis, A. and Shroff, H. (2013). Instant super-resolution imaging in live cells and embryos via analog image processing. *Nat. Methods* **10**, 1122–1126.
- Zhong, M.-C., Wei, X.-B., Zhou, J.-H., Wang, Z.-Q. and Li, Y.-M. (2013). Trapping red blood cells in living animals using optical tweezers. *Nat. Commun.* **4**, 1768.
- Zomer, A., Maynard, C., Verweij, F. J., Kamermaans, A., Schäfer, R., Beerling, E., Schiffelers, R. M., de Wit, E., Berenguer, J., Ellenbroek, S. I. J. et al. (2015). In Vivo imaging reveals extracellular vesicle-mediated phenocopying of metastatic behavior. *Cell* **161**, 1046–1057.